Techno-economic analysis of natural and stimulated geological hydrogen

Yashee Mathur
Department of Energy Science and Engineering
Stanford University
yashee@stanford.edu

Henry Moise
Department of Chemical Engineering
Stanford University
hmoise@stanford.edu

Yalcin Aydin
Graduate School of Business
Stanford University
yalcin@stanford.edu

Tapan Mukerji
Department of Energy Science and Engineering
Stanford University
mukerji@stanford.edu

Version: Jan 2nd, 2024

This is a non-peer-reviewed preprint submitted to EarthArXiv. This paper is submitted to the International Journal of Hydrogen Energy for peer review.

Abstract

Geological hydrogen has emerged as a low-cost and low-carbon primary source of energy. This study provides a comprehensive techno-economic analysis of natural geological hydrogen (GH) and stimulated geological hydrogen (SGH) production, reaffirming its potential as a low-cost energy source. For the United States, we estimate production costs at $0.54/kg for GH and $0.92/kg for SGH, demonstrating the feasibility of achieving production below $1/kg under optimal conditions. Detailed sensitivity analyses reveal hydrogen purity and production flow rates at the well head as primary cost drivers along with final delivery pressure of hydrogen. Although, GH has lower cost, SGH's scalability, driven by ubiquitous iron-rich rocks and controlled production rates, positions it as a practical solution for co-locating near demand centers. These findings underscore the potential of geological hydrogen to contribute significantly to a sustainable energy future, provided further field data validates the underlying assumptions.

1) Introduction

Energy demand is ever-increasing while the world faces the challenge of transitioning to clean sources of energy to mitigate climate change. Energy independence, security, and the quest to lower GHG (greenhouse gas) emissions are pressing issues globally. Hydrogen can supplant the role of hydrocarbons in many sectors [1], [2] due to its gravimetric energy density, clean combustion, long-term energy storage capabilities, and potential for low CO_2 production. As per the IEA Net Zero Roadmap 2021, the demand for hydrogen is expected to grow five-fold from 94 MT in 2021 to 530 MT by 2050. Currently, only 4% of total hydrogen produced globally is low-carbon green hydrogen, with a large proportion being produced by steam-reformation (78%) with or without carbon capture, and from coal (18%) [3]. Hydrogen occurs naturally in the subsurface generated by geological processes and the presence of geological hydrogen has been confirmed in various exploration campaigns around the world. Geological hydrogen is a carbon-free, sustainable resource, representing a new source of clean energy for the future. Despite the potential game-changing impact on clean energy and the environment, natural H_2 exploration and production from the subsurface is still in the early stages and has not been implemented globally. We lack a detailed understanding of the techno-economic and environmental impacts of various geological H_2 extraction schemes, limiting our understanding of their role in the future energy system. The objective of this study is to explore the techno-economic cost drivers for both naturally occurring and stimulated geological hydrogen production, aiming to understand the factors influencing the production cost of hydrogen to truly unlock the low-carbon geological hydrogen economy.

The Earth hosts vast resources of naturally occurring hydrogen [4] in different geological environments with an estimate of 23 MT/year annual flow of hydrogen from all geological sources. Natural hydrogen has been observed in many different geological environments including but not limited to ophiolites [5]–[9], continental rifts, back-arc basins, intracratonic basins, cratonic areas, and ore deposits [10], [11]. Analysis [12] suggests that the current H_2 production potential of the Precambrian continental lithosphere has been underestimated and the estimate of H_2 production rates from the Precambrian continental lithosphere is closer to $0.36–2.27 \times 10^{11}$ moles/year (73-458 kta). The primary source of all hydrogen is primordial and was generated during the formation of Earth and the solar system, where it was initially captured and then dissociated to form a hydritic core and lower mantle during the formation of the Earth [13]. Other studies also indicate that

hydrogen could largely be present in the Earth's core [14], [15]. Natural hydrogen can be regarded as having either an abiogenic or a biogenic source, of which the latter includes both thermogenic and microbial processes [16]. Hydrogen produced from biogenic sources along with natural gas has been encountered during oil and gas exploration. Abiogenic sources such as serpentinization and radiolysis are considered the main secondary sources of hydrogen [16], [17]. The term *serpentinization* generically describes the hydrothermal alteration of primary ferromagnesian minerals such as olivine ($(Mg, Fe)_2SiO_2$) and pyroxenes ($(Mg, Fe)SiO_3$) (generally referred to as ultramafic rocks), which may produce serpentine group minerals depending on pressure/temperature (P-T) parameters. Oxidation of Fe^{2+} in olivine and pyroxenes leads to the reduction of water and the formation of molecular hydrogen. Another important reaction for hydrogen production is the radiolysis of water by alpha, beta, and gamma radiation released in the radioactive decay of U, Th, and K-bearing minerals [11].

The current estimates of hydrogen potential are still low considering that the formation of aqueous hydrogen is thermodynamically feasible and expected to form virtually everywhere where iron-rich rocks such as olivine and water interact [18]. The Earth's crust comprises 10% of olivine compounds. Even if naturally occurring hydrogen is not generated at requisite rates in the sub-surface, it can be further stimulated using water, heat and other catalysts [19]. Moving forward, for brevity, we refer to hydrogen produced naturally without any extrinsic intervention as geological hydrogen (GH) whereas hydrogen produced by further stimulation of the subsurface via any kind of permeability enhancement techniques as stimulated geological hydrogen (SGH). Recently, there has been a growing impetus to understand the overarching reactions and mechanisms through which hydrogen can be produced via stimulation of iron-rich rocks owing to the estimates that greater than 100 trillion tonnes of hydrogen can be produced via these processes [19].

Hydroma (formerly Petroma) struck 98% pure hydrogen in Bougou-1 well in the Bourabougou field in Mali, Africa while exploring for water in 1987 [20] followed by drilling 24 wells across an area of 780 km^2 with a production of 1500 m^3/day from the first reservoir [21]. Moreover, in the 11 years of production from the first well that supplies electricity to the village, there has been no pressure decline whatsoever but rather a slight pressure increase from 4.5 to 5 bars [22]. The possibility of a potentially endless low-carbon energy resource with low costs of production has stirred the exploration of natural hydrogen. The Bourabougou discovery might be considered a tipping point for natural hydrogen like the Drake well in Pennsylvania in 1859 that started the “black gold rush”.

The lower cost of producing natural hydrogen and its low environmental impact have made it an attractive green energy alternative. A recent study on the lifecycle assessment of natural hydrogen shows that it is expected to produce 0.4 kg equivalent of CO_2/ kg H_2 [23] as compared to 9-13 kg of CO_2/kg H_2 produced by steam-methane-reformation [3]. Consequently, companies exploring natural hydrogen have sprung up in multiple regions around the world including in the USA, France, Spain, and Australia [24]. Natural geological hydrogen has been claimed to be produced at a cost of below $1/kg [20], but there is limited public data detailing how this can be achieved. For stimulated hydrogen, The U.S. Department of Energy has set production targets for $1/kg for hydrogen at the wellhead with <0.45 kg CO_2/kg H_2 produced.

We conduct a comprehensive analysis of the capital expenditure (CAPEX), and operating expenditure (OPEX) costs associated with producing geological hydrogen through both natural accumulations and stimulation methods. A roadmap for the rest of the paper is as follows. In section 2 we describe the multifaceted geological hydrogen value chain, including the upstream, midstream and downstream segments. Section 3 identifies the upstream costs associated with exploration and development. The midstream costs associated with surface processing, purification and compression are delineated in section 4. This is done separately for GH and SGH production processes. Section 5 then utilizes the various costs identified in sections 3 and 4 and performs a techno-economic analysis. A sensitivity analysis is also performed to identify the factors that most impact the cost of geological hydrogen production. This is followed by discussions on storage and transportation requirements (section 6) and downstream end use (section 7). Environmental impacts and policy frameworks constitute section 8, followed by discussions and conclusions.

2) The geological hydrogen value chain

The geological hydrogen industry like any other subsurface resource industry will encompass a complex and multifaceted value chain (Figure 1). This would be further divided into upstream, midstream, and downstream segments each playing a critical role in transforming hydrogen for varied end-use cases.

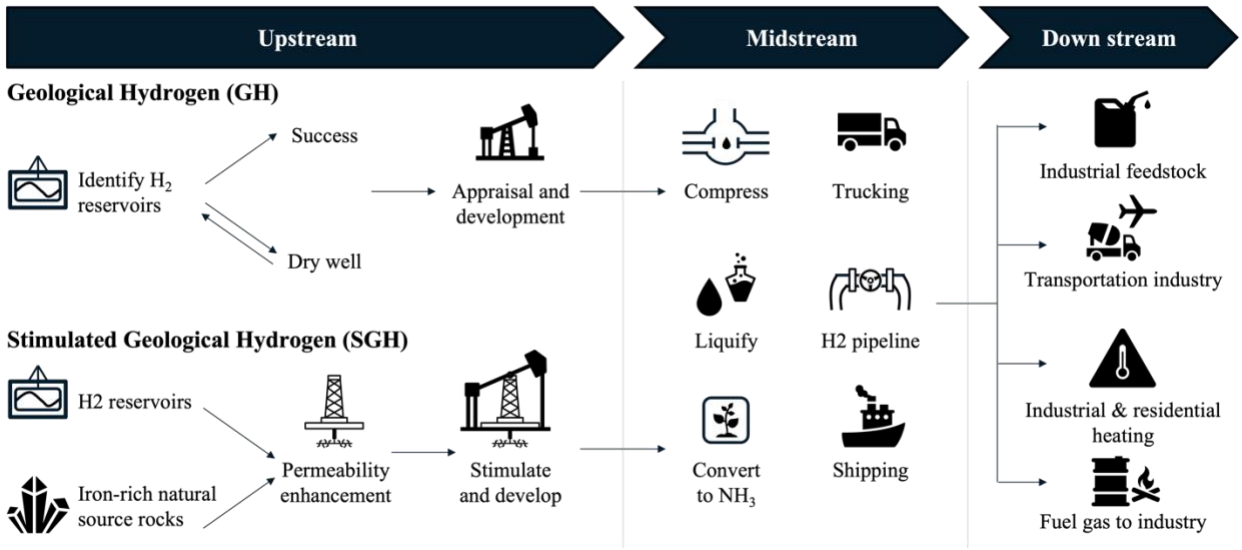

Figure 1: The geological hydrogen value chain comprising upstream, midstream and downstream components

The upstream segment, also known as the exploration and production (E&P) phase, involves the identification, extraction, and initial processing of hydrogen. Natural geological hydrogen can be extracted directly from reservoirs that host vast accumulations of hydrogen or are continuously being replenished by a nearby source. These reservoirs can be produced via standard drilling techniques used in oil and gas or geothermal extraction. Examples include projects in Mali [20], [22] by Hydroma and Gold Hydrogen in Australia. On the other hand, stimulated or enhanced

geological hydrogen would encompass hydrogen resources that would be produced directly from hydrogen-generating source rocks.

The midstream segment covers the surface processing-purification, compression, transportation, storage, and wholesale marketing of hydrogen. This segment includes pipelines, storage facilities, and distribution networks essential for moving hydrogen from production sites to end users. Today transportation of hydrogen is done by tube trucking, liquid phase trucking, and via pipelines. Storage facilities, including tank farms and underground storage, are necessary for managing supply and demand fluctuations, ensuring a stable supply chain.

The downstream for hydrogen encompasses its utilization in diverse end-use applications. Hydrogen has varied use cases but is mainly used today in industrial processes for ammonia production and refining. More near-term uses include green steel production and power and heat generation via combustion and fuel cells. As a potentially low-carbon and low-cost reducing agent, hydrogen is often considered the "Swiss Army Knife" for decarbonization and GH has the potential to unlock more use cases for hydrogen and make the existing ones more cost-competitive.

3) Upstream - Exploration, Appraisal and Development

In this section, we identify and outline the major costs in the upstream segment of the hydrogen value chain. The exploration of GH is a capital-intensive endeavor and entails multiple processes. First and foremost is securing the rights to explore and potentially produce from a specific area which could involve negotiating leases with landowners or governments. This is followed by geological and geophysical studies that might include magnetic and gravity surveys. Remote sensing data analysis and detailed geological mapping can also be carried out with geochemical soil gas sampling to detect any surface expression of hydrogen. Exploration culminates in drilling wildcat wells, which involves site preparation, rig costs, drilling fluids, casing, logging, testing, and flowback analysis to confirm the presence of hydrogen. Additionally, a successful discovery entails a flow-back test to understand the production potential of hydrogen and establish flow rates. In the case of SGH, there would be additional capital and operating expenditure related to horizontal drilling and permeability enhancement.

The results of the exploration provide a go-no-go signal and if the project succeeds it proceeds to the next phase – appraisal. This involves drilling additional wells to de-risk prospective resources and decrease the geological uncertainty. This can entail acquiring more geological and geophysical data such as a 2D or 3D seismic survey, interpretation, and extended well testing. This could also entail in some cases drilling a commercial well that can be hooked up for production. In the case of stimulated hydrogen additional monitoring wells can be drilled to understand better the reactions progressing in the subsurface. Other costs in the exploration phase include royalties to lease owners or the government, insurance costs, and costs related to health, safety, and environmental compliance. Moreover, there are operational costs such as maintenance and costs associated with training and employing personnel responsible for all the upstream activities.

Table 1 summarizes estimates of the major capital expenditures in the upstream segment with sources for those estimates. Please note that these costs are valid for the United States and can vary with different regions, countries and locations. All costs are on a per well basis. The test drill

includes all the prior geological and geophysical exploration activities that culminate in this drilling. Test drill here refers to the geotechnical drilling to establish the presence of hydrogen. The test drill might not be required for subsequent appraisal and development wells. Since a naturally occurring geological hydrogen deposit would be difficult to find and has the risk of encountering a dry well, the base case chance of success is taken to be 20% - motivated from conventional oil and gas exploration where the chance of success ranges from 5-20%. The sensitivity analysis in section 5 explores the impact of a range of chance of success. SGH on the other hand will be produced from iron-rich rock formations that are easier to encounter and have surface outcrops elevating its chance of success to 80% analogous to unconventional gas deposits. Fixed filing and permitting costs are taken based on the geothermal benchmarking from the US Bureau of Land Management. Currently there is no leasing pricing structure established for geological hydrogen; thus, the exploration rights acquisition cost is again benchmarked with the geothermal leasing rates. The drilling and completion costs have significant variations depending on the region, state, and country the deposit would be in, the access to infrastructure, availability of drilling and completion equipment in that region, depth of drilling, formation type that is being drilled, and cost of labor to name a few. Here, we take an average drilling cost of $4M for a natural geological hydrogen well based on geothermal benchmarking as reported by [25]. SGH has an additional cost of stimulating the formations through any permeability enhancement techniques such as hydraulic fracturing, electrical, mechanical or biological stimulation.

Cost line items	***Geological hydrogen (GH)***	***Stimulated Geological hydrogen (SGH)***
Test drill	*$500,000*	*$500,000*
Chance of success	*20%*	*80%*
Fixed filing permitting fees	*$905*	*$905*
Average acre per well	*500*	*500*
Exploration rights acquisition per acre	*$3*	*$3*
Land acquisition cost	*$1500*	*$1500*
Drilling and completions	*$4M*	*$6.7M (inclusive of cost of fracturing)*

Table 1: Summary of upstream CAPEX costs on a per well basis for base case model (costs taken for United States)

4) Midstream- Surface processing, purification and compression

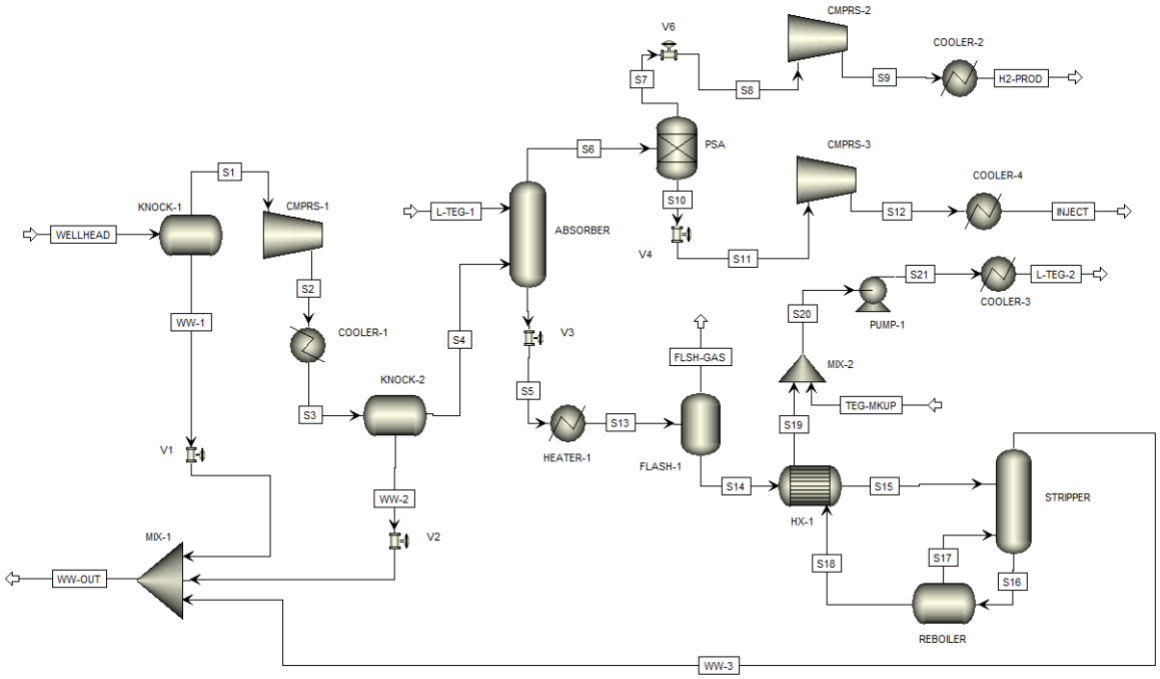

Figure 2: *Process flow diagram for surface-level processing of geological hydrogen (GH) at a single wellhead, modeled in Aspen Plus to support production rates exceeding 20 kta H_2. Key unit operations include condensate removal, gas dehydration, purification via pressure swing adsorption (PSA), and multi-stage compression, producing a hydrogen stream with >99% purity*

After the hydrogen exits the well, it needs to be refined, purified and compressed for either further transportation, conversion into other molecules or end use cases. In this section, we elaborate on the steps for the purification and compression of hydrogen and the costs associated with it. All of the processes outlined here are covered under the operating expenditure (OPEX) of a natural hydrogen processing facility. Due to limited commercial demonstrations, public data on the extraction and processing of raw geological hydrogen (GH) is scarce. Nonetheless, the established techniques and systems for natural gas (NG) processing can serve as a useful proxy when anticipating the processes required for GH processing. The process flow diagram proposed and modeled in this assessment using ASPEN Plus (Figure 2) is primarily inspired by current practices and technologies utilized in NG processing, with some modifications informed by preliminary field reports on typical site conditions for GH [10], [20]. The energy and mass balance for the overall process modeled in ASPEN Plus is summarized in Fig- S.3.

Once extracted from a wellhead, raw NG must be processed and refined onsite to meet certain regulatory and safety standards before it can be injected into a liquified natural gas (LNG) pipeline [26]. Although site specific, raw NG exiting a wellhead can contain varying levels of adulterants such as water vapor, C_{2+} hydrocarbons (natural gas liquids - NGLs), inert gases, carbon dioxide, and hydrogen sulfide. The elimination or reduction of these contaminants down to certain concentrations is well defined for NG as they are critical in ensuring the safe (and economical) storage, transport, and utilization of the commodity – no such regulations or mandates exist for GH refinement. Pipeline quality specifications for hydrogen transport is still an evolving area as there exists only 1,600 miles of hydrogen pipelines throughout the United States – mostly consolidated around the Gulf coast for refineries [27]. The degree to which GH will have to be

refined will depend on its speculated end-use, but the permissible concentrations of these contaminants should be assumed to at least meet the existing standards laid out by the various federal and state agencies charged with regulating NG transport. Table 2 outlines the typical range of NG specifications required for injection into an LNG pipeline.

Parameter	***NG Specification***
Water Content	*4-7 lbm H_2O/MMscf gas*
Hydrogen Sulfide Content	*4-16 ppmv/100 scf*
Gross Heating Value	*950-1200 Btu/scf*
Total Sulfur Content	*8-320 ppmv/100 scf*
Carbon Dioxide Content	*2-4 mol%*
Oxygen Content	*0.01 mol%*
Nitrogen Content	*4-5 mol%*
Total Inert Content (includes CO_2)	*4-5 mol%*
Delivery Temperature	*Ambient*
Delivery Pressure	*400-1200 psig*

Table 2: Typical LNG pipeline specifications for [26].

Under most operating pressures, NG has roughly 4 times the energy density of hydrogen for a given volume (Figure S.1). If the GH product were to be transported via pipeline, this lower energy density might be offset by its 3.5x larger erosional velocity compared to NG, which would enable a proportionally faster volumetric flowrate [28], [29]. Tube trailers and other compressed gas cylinders cannot exploit this feature and must rely on increased pressures to match the power delivery of NG. The transportation of compressed hydrogen is routinely achieved at pressures greater than 4x the range outlined in Table 2, but this also means 4x the material and its contaminants in a given volume [30]. As an attempt to anticipate the safe concentrations of contaminants in the GH product refined in our process, we self-imposed contaminant limits at least 4x lower than those outlined in Table 2. Beyond meeting these specifications, this work is agnostic of whether the GH product is blended into existing LNG pipelines, requires new pipelines, or uses tube trailers for its transport and only considers the delivery pressure leaving the proposed GH processing plant.

a) Natural Geological Hydrogen Process Modeling

The refinement of GH at the surface is modeled in ASPEN Plus using the Peng-Robinson property package. Well reports from different GH deposits demonstrate that a wide range of gas compositions can exist for GH deposits and choosing which composition to model for GH refinement is somewhat arbitrary. Higher concentrations of hydrogen favor the economic viability of the process and lower concentrations of hydrocarbons favor the carbon intensity of the hydrogen product [23]. The raw GH exiting the wellhead is modeled to be 75 vol% H_2, which is moderately high but also within the range of hydrogen concentrations reported in areas chosen for commercial demonstrations: Mali [20], Oman [6], and U.S. [31]. The remaining raw GH mixture consists of N_2 (12 vol%), CH_4 (9 vol%), CO_2 (2 vol%), and H_2O (2 vol%). While species like H_2S are commonly found in NG reservoirs, they have not been detected in most GH sites reported in literature [31]. Although not modeled in this work, helium is often found in GH deposits, which would introduce operational challenges in its separation if found in sufficiently low concentrations due to its inert nature. The separation and recovery of any helium contaminants is not unique to

GH though, as the need regularly arises in NG refinement [32], [33]. Although helium is in high demand, economics demand that its concentrations generally be in the excess of 0.5 vol% for a helium recovery unit to improve the NG plant economics [34]. It is unclear as to what this lower bound concentration is for GH and its separation is not modeled in this work as its production is not induced by stimulation.

i) Condensate Removal

Wells typically produce raw NG under conditions that are either below the dew point temperature or above the saturation pressure of some of its constituent gases, resulting in liquid condensate entrainment in the gas stream. These liquids can erode and foul downstream equipment which generally makes their removal the first separation step in NG refinement. The bulk of these liquid condensates can be removed using simple and cost-effective techniques such as gravity separation and slug catchers, which rely on the principles of momentum, gravity, and coalescence to separate phases. The GH well modeled in this work is assumed to be void of NGLs due to their limited presence in field measurements. Liquid water condensates are, however, expected to be present and must be removed first.

Raw GH gas leaves the wellhead at 7 bars before entering a gravity-driven two-phase separator (*KNOCK-1*, Figure 2) to remove bulk condensates from the gas stream - namely water as the gas does not contain any NGLs. The gas stream exiting this two-phase separator is then compressed to 30 bars for downstream operations, which further condenses any water vapor still in the gas stream, requiring a second two-phase separation (*CMPRS-1*, Figure 2). The liquid water that accumulates in the settling sections of the two-phase separators is eventually pumped to a wastewater storage and/or treatment area (*WW-OUT*, Figure 2), with an associated cost of \$10/m^3 wastewater [35]. Due to its low solubility in water, hydrogen losses during water condensate removal are minuscule (0.1 vol% in wastewater).

ii) Gas Dehydration

Despite removing almost 90% of the original water mass leaving the wellhead with the two-phase separators, further dehydration is required. Residual water content not only lowers the heating value of the hydrogen product, but it can also react with sour gases like H_2S and CO_2 to produce corrosive acids that would foul downstream process equipment. Under certain operating conditions, water can react with methane to form hydrates which are ice-like solids capable of clogging valves and piping [26]. These risks can be mitigated by removing sufficient water vapor and lowering the streams dew point in a process known as dehydration. Several methods exist for NG dehydration which include absorption, adsorption, direct cooling, membrane, and supersonic processes [36], [37]. Each technique has unique challenges and benefits, making their implementation dependent on specific site conditions and process demands. The most common and robust industrial technique for NG dehydration is liquid glycol absorption in a contact tower, typically using triethylene glycol (TEG) as the sorbent [38]. Since it is reasonable to expect this technique to maintain its efficiency under a largely hydrogen atmosphere, TEG absorption was selected as the optimal dehydration method for this process.

Although not necessary in our process, any NGLs present in the raw GH gas would have to be removed prior to entry into the TEG dehydration unit, which would increase fouling and carbon emissions. The H_2O-rich gas enters the bottom of the TEG dehydration contact tower (*ABSORBER*, Figure 2) at 30 bar, where it flows upward through a series of 5 trays which enhance contact between TEG and the counter current gas. The H_2O-lean gas exits from the top of the tower while the H_2O-rich TEG, which also absorbed some CO_2 and CH_4, is sent to a stripping column for regeneration. A valve (*V3*, Figure 2) reduces the pressure of the exiting H_2O-rich TEG to 7 bar before it is heated to 120°C for flash removal of condensates in a flash drum (*FLASH-1*, Figure 2). The flash gas may be recovered as a fuel in some operations but is too lean in combustibles for this process. After passing through a heat exchanger (*HX-1*, Figure 2), the H_2O-rich TEG enters a stripping column (*STRIPPER*, Figure 2) at 190°C to produce a gas stream of H_2O (64 vol%), CO_2 (21 vol%), and CH_4 (11 vol%). The H_2O-lean TEG regenerated in the stripping column passes through a reboiler (*REBOILER*, Figure 2), operated just under the decomposition temperature of TEG (208°C), to produce a 96 vol% TEG stream for recycling. The water that has been stripped from the gas is considered wastewater and is sent to the same wastewater storage area produced by condensate removal process (*WW-OUT*, Figure 2). After heat-exchanging with the H_2O-rich TEG entering the stripping column, the H_2O-lean TEG is mixed with make-up TEG (*TEG-MKUP*, Figure 2) to account for any decomposition and vaporization losses. The H_2O-lean TEG mixture is then pressurized to 30 bar and pumped back into the TEG contact tower TEG (*L-TEG-1/2*, Figure 2).

iii) Dry Gas Purification & Compression

The gas exiting the dehydration unit is adequately dry, but significant concentrations of methane, nitrogen, and carbon dioxide remain, necessitating further purification before the gas can be sold. Several technologies are currently employed at scale that can accomplish separating these gases from the hydrogen product, including absorption, adsorption, membrane, and cryogenic processes. Each technology is employed depending on the economics of the well's gas mixture and the demands of the process, which makes their utilization in NG and GH site-specific.

In traditional NG processing, separating methane from the gas mixture is accomplished through a series of operations which can include acid gas removal units, nitrogen rejection units, and cryogenic distillation among others. Due to the similarities in molecular size between methane (3.8 Å) and nitrogen (3.6 Å), and a similar affinity to many adsorption materials, cryogenic distillation is favored for NG refinement. Engelhard developed a titanium silicate molecular sieve designed with a 3.7 Å pore size capable of selectively adsorbing nitrogen in a pressure-swing adsorption (PSA) unit, but its application is limited to flowrates of 0.5-1 MMscfd [39]. Less selective PSA units are generally limited to wells producing up to 15 MMscfd, while membranes can work up to 25 MMscfd [26]. Having hydrogen as the desired product instead of methane brings about significant advantages when it comes to gas separation. Outside of helium, hydrogen has the smallest molecular size and the lowest affinity for adsorption materials of any gas encountered in crude GH gas mixtures – making membrane and PSA separation technologies more economically viable for GH. Specifically, PSA technologies are superior in industrial hydrogen separation as they are almost exclusively used in steam-reforming, which produces 78% of the world's hydrogen. Given that the production rate of the well modeled in Figure 2 is close to the 15 MMscfd threshold for NG PSA units, hydrogen separation was simulated using a PSA.

The H_2O-lean gas that exits from the TEG dehydration units enters the PSA (*PSA*, Figure 2) at 30 bar, which experiences a pressure drop of 3 bars and recovers 80% of the hydrogen at a 99.2 vol% purity. This pure hydrogen product stream then enters a compressor (*CMPRS-2*, Figure 2) to recuperate the pressure lost in the bed as well as meet the required pressure for transportation; the value of which will be varied to meet each form of transport. The off-gas (*S10*, Figure 2) desorbs from the bed at atmospheric pressures and consists of methane (23.5 vol%), nitrogen (31 vol%), carbon dioxide (5 vol%), and the non-recoverable hydrogen (40 vol%). This off-gas may serve as a fuel, but the high concentration of nitrogen may result in unstable combustion. For this reason, the off-gas is compressed (*CMPRS-3*, Figure 2) to wellhead pressures for re-injection.

b) Stimulated Geological Hydrogen Process Modeling

Similar to the refinement and processing of GH, stimulated geological hydrogen (SGH) has not been commercialized and its anticipated operation will have to draw inspiration from more mature technologies like hydraulic fracturing, enhanced geothermal systems, and water flooding for secondary oil recovery. The refinement and processing of SGH at the surface is not expected to differ from GH, aside from the potentially elevated partial pressures of water leaving the wellhead that may arise from incomplete serpentinization reactions. From this assumption, the OPEX costs associated with SGH can simply be appended onto those for GH.

i) Water Injection

The exothermic serpentinization reaction that produces the hydrogen requires moderate operating temperatures of 200-300°C [18], which will determine the minimum depth of drilling and the economic viability of the deposit. Due to the large, perpetual thermal mass of the subsurface at these depths, steam generation prior to injection is not needed as it will be generated in-situ through conductive heat transfer. Pumping water as opposed to generating steam shifts the primary cost of water injection towards the source of the water itself. Fortunately, literature suggests that the source and quality of this water is not prohibitive in its utilization [40], [41]. The deployment of non-potable water sources like seawater, brackish water, and reclaimed wastewater would alleviate OPEX costs as well as increase the operational footprint of these operations to encompass more water-scarce regions. The cost of these water sources will vary seasonally and geographically, but general ranges for viable sources can be found in Table 3.

Water Source	***Cost [$/m^3]***
Industrial Water	*0.25-5*
Brackish/Sea Water	*0.01-0.1*
Reclaimed Wastewater	*0.1-0.5*

Table 3: Range of costs for potential water sources used in this work.

Unlike traditional reaction engineering, geo-engineering these subsurface "reactors" means limited influence on their operating parameters due to the fixed temperatures and pressures at these depths. Drilling deeper into the geothermal gradient will provide higher temperatures and improved serpentinization rates, but at the expense of increased drilling costs. In places where the suitable iron-rich rocks are encountered at a shallower depths like Oman [5], the natural geothermal gradient might not be enough to reach the requisite serpentinization temperatures. In cases like

this, to manipulate temperatures, steam injection [42] would be another feasible methodology to enhance the serpentinization rates. Another possible parameter that can be manipulated is the catalytic activity of the water being injected. Any catalyst co-fed with the water into the subsurface is not likely to be recovered, limiting options to cheap and consumable chemicals like NaOH, HCl, and NaOH – all of which have been demonstrated to catalyze the serpentinization reaction [43]. As commodity chemicals, their widespread use in various industrial processes means that existing supply chains and infrastructure can be leveraged to support large-scale operations. Assuming these chemicals can be employed at scale without environmental concerns, their ease of handling and storage also simplifies logistics and makes them practical choices for field operations. While it is expected that the concentration of these chemical co-feeds will be site-specific, their addition modeled in this work will be fixed at the concentrations tested in literature – namely 0.5M NaOH, 0.5 NaCl, and 0.05 HCl [43]. Their bulk costs can be found in Table 4.

Chemical Co-feed	***Cost [$/kg]***
NaOH	*0.2-0.4*
NaCl	*0.15-0.25*
33 wt% HCl	*0.05-0.2*

Table 4: *Range of costs for chemical co-feeds used in this work.*

ii) Water Containment & Reaction in the Subsurface

The primary cost drivers of SGH in the subsurface can be distilled down to two aggregate terms: the extent of water that is contained within the injection volume and the extent that participates in the serpentinization reaction. The maximum amount of hydrogen that can be extracted from the injected water is 0.112 kg H_2/kg H_2O, and this value decreases proportionally when either of these two terms decrease. Both values are aggregates that actually encompass several site-specific and compounding variables which include the concentration of Fe(II) minerals in the formation, its permeability and porosity, rate of the serpentinization reaction, and the presence of microorganisms that oxidize the produced hydrogen gas via hydrogenases [44]. Assigning values to either aggregate term will rely heavily on assumptions without more public data and site-specific field demonstrations to guide some of the reasoning.

Lab-scale demonstrations of SGH are constrained in scope but have effectively stimulated a variety of source rocks under relevant conditions and time periods - often operating over several weeks to several months to achieve steady-state hydrogen generation. Reported production rates can vary from one another substantially, sometimes by orders of magnitude from field measurements [45]–[47] - highlighting the intrinsic challenge of assigning singular values to production rates in this work. From the lab-scale experiments, a steady state production rate of 1 kg H_2/m^3 source rock seems achievable under their idealized conditions, which is 25% of the 4 kg H_2/m^3 maximum yield of peridotite-type rocks. While these experiments did not replicate the surface area or heterogeneity of rocks that will be encountered in field stimulation, they establish a preliminary ceiling for achievable production rates until more public data become available. It is anticipated that the fracture spacings induced in the field and the reactive surface areas they generate will be orders of magnitude lower than those studied in the lab [48]. In anticipation of less ideal stimulation conditions in the field, this work assumes that the efficiency of serpentinization, defined as the

percentage of the maximum yield achievable by peridotite-type rocks (4 kg H_2/m^3), can range from 0.1-25% (0.004-1 kg H_2/m^3), with a base case value of 15%.

Defining the containment efficiency of water within the injection volume requires a range of values to account for variability between potential sites and their formation characteristics. Guidance can be drawn from other subsurface fluid injection processes, such as hydraulic fracturing, enhanced geothermal systems, and water flooding for secondary oil recovery. Recovery of injected water is lowest in hydraulic fracturing, with only 10-30% recovered during flowback. Enhanced geothermal systems, which are more like SGH, achieve recovery efficiencies of 90-95% [24]. Although SGH does not aim to recover injected water, recovery efficiency indirectly indicates how much water remains in fractures. The volumetric sweep efficiency of waterfloods, defined as the ratio of reservoir volume contacted by the injected fluid to the total reservoir volume, ranges from 40-60%. This metric serves as a proxy for how effectively injected water reaches fractures in SGH. Enhanced geothermal systems provide a closer analogy to SGH due to their focus on fluid recovery, while hydraulic fracturing, optimized for hydrocarbon extraction, bears the least resemblance. Containment efficiencies below 40% raise concerns about sustainability and responsible water use. Therefore, the modeled containment efficiencies range from 40-95%, with a base case of 80%.

5) Techno-economic analysis and sensitivity

In this section, we utilize both CAPEX and OPEX costs mentioned in section 3 and 4 and with additional assumptions calculate the cost of hydrogen per kg and identify the factors that are most sensitive to the cost of hydrogen.

The reported hydrogen concentrations in the literature range from <1% to up to 98% in Mali [20] and 56% and 37% H_2 reported in historic oil and gas wells in Kansas [31]. Utilizing this public data, the base-case wellhead gas concentration was chosen to be 75% H_2. This choice hopefully avoids being overly optimistic while still being high enough to minimize the potential emissions associated with lower concentrations if the balance gases are hydrocarbons [23]. While individual wellhead production flowrates are not publicly available, this work assumes a base case value of 200 kg H_2/hr, which under the right assumptions can align with initial volumetric production rates seen in new NG wells in regions like Alberta and Texas [49]. Outlined in section 3 and 4, the energy and capital costs associated with upstream operations were incorporated into the economic model for both GH and SGH. As such, it was assumed that the delivery pressure leaving the ASPEN plus model was 30 bar and that the GH produced would be used on or near the production facility. More details on the serpentinization production rate and water containment efficiency have been discussed earlier in section 4. Additional key assumptions utilized in this analysis are summarized in Table 6.

Parameter	***Assumed Value for base case***
Well Lifetime (GH & SGH)	*20 years*
Re-hydraulic fracturing frequency (SGH)	*5 years*
Annual Operation Days (GH & SGH)	*300*
Wellhead Gas Composition (GH & SGH)	*75% H_2*

Wellhead Production Flowrate (GH & SGH)	*200 kg H_2/hr*
Delivery Pressure (GH & SGH)	*30 bars*
Serpentinization Production Rate (SGH)	*0.6 kg H_2 /m^3 source rock*
Water Containment Efficiency (SGH)	*80%*
Stimulation Water Source (SGH)	*Industrial water at \$1/m^3*

Table 6: Assumed values used in base case TEA.

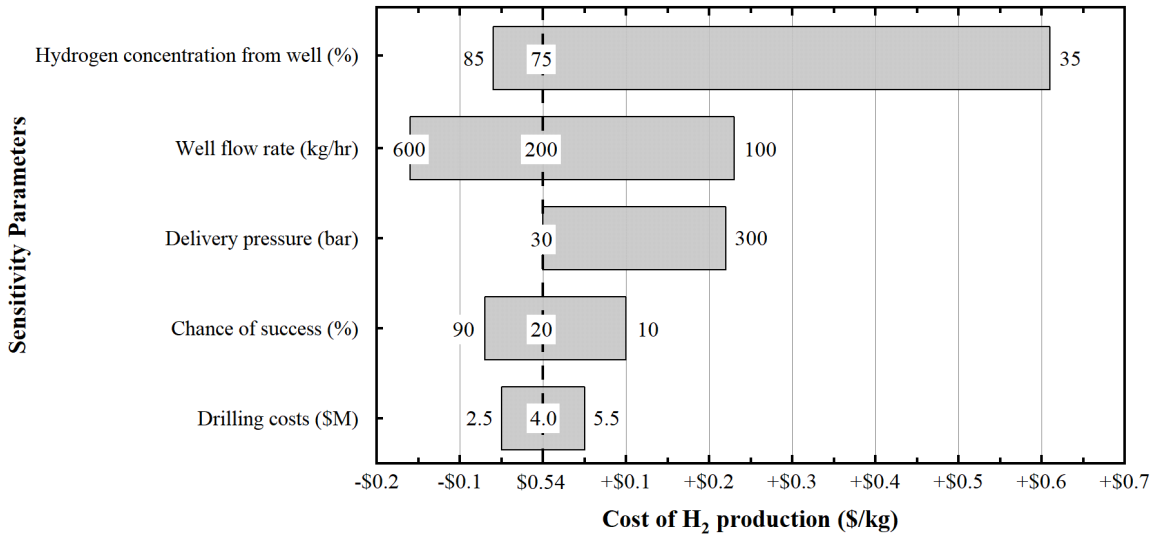

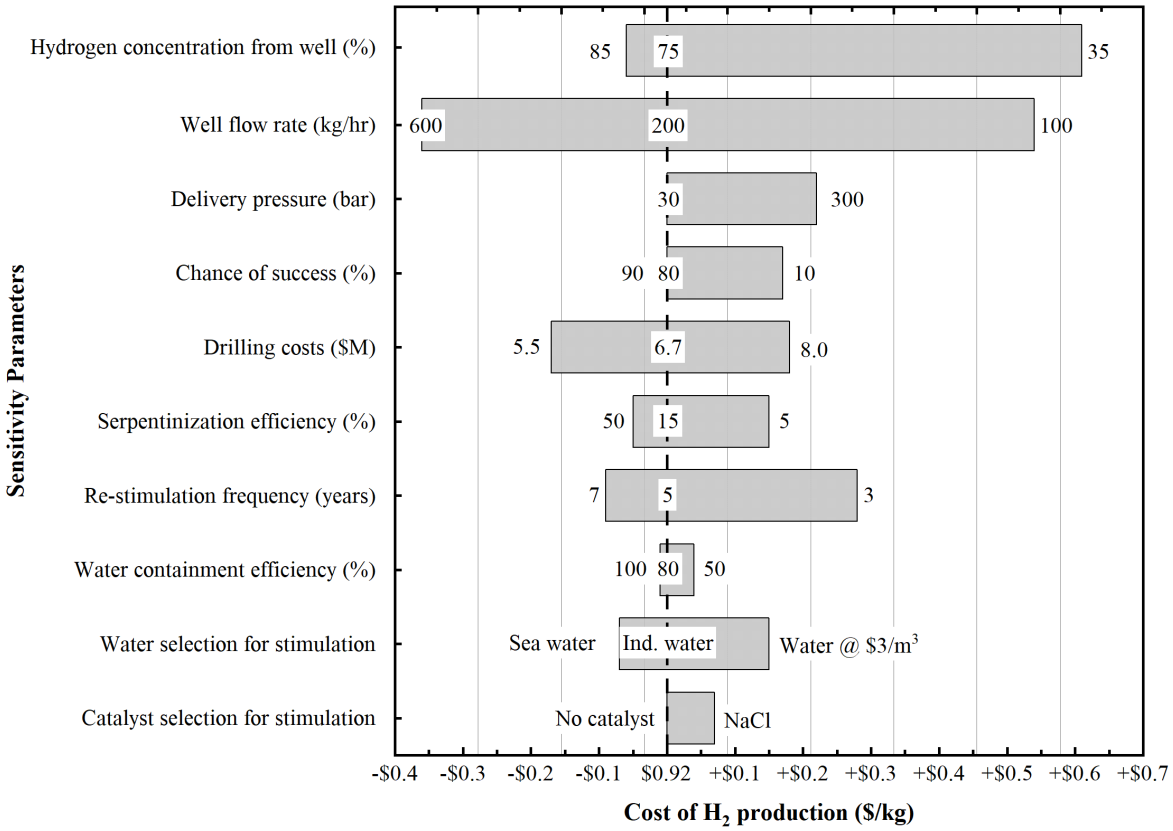

Figure 3: Sensitivity analysis for hydrogen production costs (without transport) for (top Geological hydrogen and (bottom)Stimulated Geological hydrogen. The numbers at the center are the base case and at the ends are the high and low case for each factor.

The base case techno-economic analysis results in hydrogen production cost of $0.54/kg for GH and $0.92/kg for SGH. A sensitivity analysis was performed to identify the primary cost drivers for this technology. Figure 3 outlines this sensitivity analysis in the form of a tornado plot, which as expected identifies gas purity and production flowrate as the largest cost drivers for both GH and SGH. The numbers at the center are the base case assumptions and at the end are the high and low cases for each dimension that are physically possible. Since hydrogen purity and flow rates are most impactful cost drivers, we also show the variation of hydrogen cost across a range of flow rates and purity. Naturally energy intensity increases for surface level processing as well-head purity decreases (See Fig-S.2). Figure 4 illustrates these relationships, showing the relative impact of each variable when the other is held constant. The analysis reveals that the < $1/kg H_2 cost target is achievable and that while both gas purity and flow rate significantly influence production costs, their effect diminishes beyond a certain point. For GH, achieving the $1/kg H_2 cost requires flow rates exceeding 75 kg H_2/hr and purity levels above 40%. In contrast, SGH—due to additional production-related costs—requires a higher flow rate of 175 kg H_2/hr and purity levels above 65% to reach the same price threshold. Of course, these thresholds are subject to the assumptions of this work.

Beyond wellhead gas concentration and flowrate, Figure 3 identifies delivery pressure as the next largest cost driver which was assumed to reach the 350 bar minimum requirement for most forms of hydrogen transport – adding an additional $0.22/kg H_2. Under the base case assumptions, SGH was able to achieve a cost of $0.92/kg H_2 – roughly $0.38/kg more expensive than GH due to additional CAPEX of permeability enhancement and water injection. Figure 3 also illustrates that serpentinization efficiency moderately influences the final hydrogen cost, up to an additional $0.15/kg H_2, surpassing the impact of water containment efficiency. This of course arises from the assumptions made in this work, but these assumptions stem from rates measured under idealized laboratory conditions, which often demonstrate limited utilization of the injected water. To enhance the economic viability of this technology, it will be crucial to develop techniques and disposable catalysts that facilitate greater hydrogen production rates in less-than-ideal field conditions. Furthermore, both efficiency metrics ultimately hinge on the cost of water, underscoring the importance of sourcing the most affordable water options available. The analysis assumes that industrial water will be the most readily accessible resource, particularly since the land area adjacent to seawater is considerably smaller than that of inland regions. However, projects would benefit from access to seawater and brackish water sources, which could further optimize production costs and operational efficiency. Comparable in sensitivity to serpentinization efficiency is the frequency of restimulating the deposits, which in this analysis was assumed to occur every five years. However, in practice, the frequency may vary depending on the need to expose fresh reactive surfaces or enhance permeability through the rock formations. Adjusting refracturing intervals based on real-world conditions could significantly impact operational efficiency and long-term hydrogen production rates.

So far, the analysis has shown that GH is more cost effective than SGH that has additional costs in terms of permeability enhancement, water, catalyst etc. But for practical purposes iron-rich rocks are more ubiquitous than GH deposits. Since hydrogen transportation is one of the most important

factors for the entire hydrogen economy to scale, the probability of finding iron-rich rocks near demand centers would be higher than finding GH deposits. Therefore, it would be favorable to develop a SGH project in co-location with an active hydrogen demand center. Moreover, the hydrogen flow rates from a SGH well can be controlled that would further improve the economics of the well.

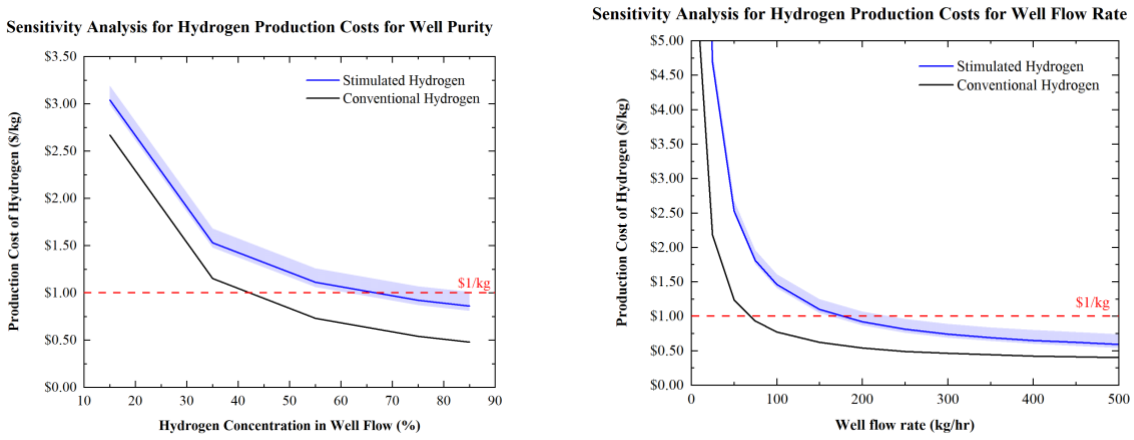

Figure 4: Hydrogen production cost (without transport) as a function of (left) production flowrate and (right) wellhead gas composition. SH is depicted in each plot as a black line while SGH is represented as a blue line with a shaded uncertainty region including the possible range of production rates ranging from 0.004-1 kg H2/m^3.

6) Transportation and storage requirements

The current study does not incorporate the transportation costs into the specific cost of hydrogen owing to the variability in total cost based on delivery distance and hydrogen throughput (Figure 5). The optimal transportation method depends on the volume of deposit, location, distance to the end user, and infrastructure availability. There is no one-size-fits-all solution. To transport large amounts of hydrogen, it must either be pressurized and delivered as a compressed gas or liquefied, depending on throughput and delivery distance [50]. Hydrogen can be transported in four primary ways: a) gaseous transport, b) liquid transport, c) hydrogen carrier materials, and d) blending with natural gas [51].

Gaseous hydrogen transport involves compressing hydrogen to high pressures and delivering it via pipelines or tube trailers. Pipelines are efficient for large-scale, long-distance continuous transport within regions with stable demand. However, they require high upfront capital investment and specialized materials to prevent hydrogen embrittlement and leakage. The U.S. currently has 1,600 miles of hydrogen pipelines in the Gulf Coast region, compared to 3 million miles of natural gas pipeline. Tube trailers are suitable for shorter distances and smaller volumes, providing flexibility where pipeline infrastructure is unavailable. Liquid hydrogen (LH2) transport is preferred for long distances and larger volumes. Hydrogen is liquefied through cryogenic cooling to -253°C and transported in super-insulated, cryogenic tanker trucks. This method offers higher energy density and efficiency for long-distance transport and provides flexibility in transportation mode (road, rail, shipping) compared to gaseous hydrogen. However, the liquefaction process is energy-intensive and costly, consuming over 30% of the hydrogen's energy content. Boil-off losses during transport also present a challenge. Various hydrogen carriers, including metal hydrides such as sodium borohydride ($NaBH_4$), ammonia, and liquid organic hydrogen carriers (LOHCs), are still

in the research phase due to challenges in scalability, regeneration, and material synthesis. These carriers offer potential solutions for hydrogen transport but require further development to be commercially viable. Blending hydrogen with natural gas (up to 20% by volume) can leverage existing natural gas infrastructure for distribution. This method allows for the gradual integration of hydrogen into the current natural gas infrastructure. However, blending requires modifications to existing pipelines and end-use equipment, particularly for higher hydrogen concentrations. Separating hydrogen from natural gas can be achieved via pressure swing adsorption, membrane separation, or electrochemical hydrogen separation, but these methods are complex and costly, limiting their feasibility.

Key challenges in hydrogen transportation include reducing costs, increasing energy efficiency, maintaining hydrogen purity, and minimizing leakage. Given these challenges, co-location with the end user or conversion into other molecules on-site, such as ammonia, methanol, or syngas, might be more feasible. These alternatives have more robust supply chains but require significant upfront capital expenditure and are viable only for large deposits that can sustain production over longer durations.

For geological hydrogen, smaller pipeline networks can be developed, such as in the Kansas-Iowa-Nebraska region, which is a hotspot for hydrogen exploration in the continental United States with access to nearby demand centers. Although this entails higher upfront capital investment, higher volumes of hydrogen could unlock economies of scale ($0.2-0.5/kg for distributing 600 tonnes per day over 300 km) [52].

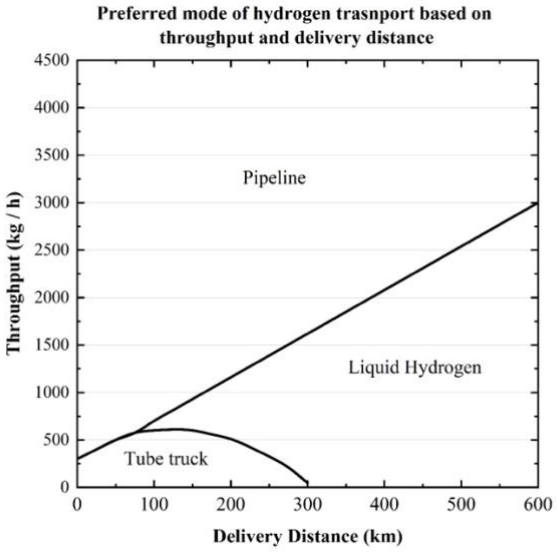

Figure 5: Preferred mode of hydrogen transport based on throughput (hydrogen produced/hr) and delivery distance of the end use case application [50]

7) Downstream

Of the 94 Mt hydrogen used in 2021, 43% was consumed by the refining industry, with the remainder used in various industrial applications. In the refining industry, hydrogen serves critical roles in purification, quality improvement, and conversion of crude oil into more valuable products

through hydrocracking. In hydrotreating, hydrogen is used to remove impurities such as sulfur, nitrogen, and metals from crude oil fractions, ensuring that the resulting petroleum products like gasoline and diesel meet stringent environmental and quality standards. In hydrocracking, hydrogen helps break down larger, heavier hydrocarbon molecules into lighter, more valuable products such as gasoline, diesel, and jet fuel, stabilizing the smaller hydrocarbon molecules formed during this transformation. In the industrial sector, hydrogen's current applications include serving as a feedstock for ammonia and methanol production, which are foundational to the chemical industry. These processes highlight hydrogen's indispensable role in supporting various industrial activities. Ammonia production, crucial for fertilizer manufacturing, accounted for about 36% of hydrogen demand in 2021. Methanol production, essential for creating plastics and synthetic fibers, required approximately 16% of hydrogen during the same period. These uses underscore hydrogen's pivotal role in the chemical industry and its potential for future expansion.

Table 5 outlines the willingness to pay per kilogram of hydrogen by various end users. Currently, most of these industries rely on hydrogen produced via steam-reformation (SR). Without external incentives to switch to low-carbon hydrogen, factors such as price and reliability are critical in deciding whether to transition from SR to geological hydrogen. To be competitive, geological hydrogen must match or undercut the price per kilogram of SR hydrogen. The cost of transportation significantly impacts the overall price of hydrogen, making proximity to demand centers a key parameter. Industrial processes such as the Haber-Bosch method for ammonia production operate continuously to maintain throughput and often have decade-long off-take agreements. For context, a small-sized ammonia plant with a 500 tonnes per day (TPD) capacity requires approximately 88.5 TPD of hydrogen. To illustrate, the Ramsey project in Australia has a prospective resource potential of 1.3 billion kilograms of hydrogen [53]. This amount could theoretically fulfill the hydrogen needs of a 500 TPD ammonia plant for approximately 40 years. However, it is important to note that this is a prospective resource potential, and actual proven reserves may be lower. Consequently, identifying high-volume deposits and ensuring continuous on-demand production is crucial for the success of geological hydrogen as a sustainable and reliable energy source.

Hydrogen Use Case	***Willingness to pay***
Ammonia	*$0.9- 2.3/kg*
Refining	*$1-1.3/kg*
Steelmaking	*$1.25-2.3/kg*
Chemicals	*$0.9-2.3/kg*
Natural Gas Blending	*$0.4-0.5/kg*
Industrial Heat	*$0.7-1.5/kg*
Power generation	*$0.4-0.5/kg*
Aviation and Maritime	*$0.7-3/kg*
Road Transportation	*$4-5/kg*

Table 5: Willingness to pay for different end use utilization of Hydrogen (*modified from* [52])

8) Environmental impacts and policy frameworks for the GH industry

Hydrogen is not a greenhouse gas itself but an indirect greenhouse gas. According to the multi-model assessment presented in [54], the 100-year time-horizon Global Warming Potential (GWP100) of hydrogen was estimated to be 11.6 ± 2.8. This means that over a 100-year period, the global warming effect of hydrogen is approximately 11.6 times stronger than that of carbon

dioxide. Emissions of hydrogen in the troposphere influence the global distributions of methane and ozone. If hydrogen were to replace the current fossil fuel-based energy system and exhibit a 1% leakage rate, it would result in a climate impact equivalent to 0.6% of the current fossil fuel-based system [55].

At the time of publication, the Inflation Reduction Act (IRA) has introduced a clean hydrogen production tax credit (PTC) of up to $3 per kilogram for hydrogen that meets stringent lifecycle emissions standards of less than 0.45 kg of CO_2e per kg of H_2 produced. Baseline geological hydrogen production is estimated to release 0.4 kg CO_2e per kg of H_2 produced [23]. The primary sources of these emissions are embodied and fugitive emissions. Emissions can increase if waste gas is flared, if operations are powered by natural gas, whether the gas mixture has a high methane (CH_4) content, or if the productivity of the well is very low. Despite this, geological hydrogen production has the lowest carbon intensity among clean hydrogen production methodologies when considering embodied emissions. The Notice of Public Rulemaking (NPRM) issued by the IRS and Treasury Department provides definitions of key terms and specifies how producers should calculate lifecycle greenhouse gas emissions using the 45V H2-GREET model. However, the current GREET model does not include geological hydrogen, presenting a gap that needs addressing for geological hydrogen to fully benefit from the 45V tax credit. To maximize the benefits from the 45V tax credit, geological hydrogen projects must ensure high purity and high production volumes. Additionally, the use of cleaner electricity, either from burning hydrogen or purchasing clean electricity from the grid, is essential. Co-locating geological hydrogen projects within DOE's regional hydrogen hubs can enhance their economic viability by leveraging existing infrastructure and ensuring a stable demand.

Summary and discussion

This study provides a comprehensive techno-economic analysis (TEA) of both natural geological hydrogen (GH) and stimulated geological hydrogen (SGH), focusing on understanding the cost drivers, feasibility, and scalability of hydrogen production through both natural and enhanced means. The goal of this analysis is to assess the economic viability of geological hydrogen as a low-carbon energy source, focusing primarily on the upstream costs related to exploration and extraction and surface processing costs when hydrogen exits the well head.

The techno-economic analysis reveals that the base case production cost for natural geological hydrogen is estimated at $0.54/kg, while stimulated hydrogen production costs approximately $0.92/kg. Despite the higher costs associated with SGH due to additional processes like permeability enhancement and water injection, both GH and SGH remain economically attractive compared to other low-carbon hydrogen production methods such as electrolysis or SR with carbon capture. The analysis shows that achieving a production cost below $1/kg is feasible for both GH and SGH, provided hydrogen purity and flow rates exceed specific thresholds. Under the assumptions used in this study, GH requires a flow rate exceeding 75 kg H_2/hr and a purity level above 40%, whereas SGH will require flow rates of 175 kg H_2/hr and purity levels exceeding 65% due to its increased costs of production. The paper also highlights that hydrogen purity and production flow rates are the primary cost drivers for both GH and SGH. Sensitivity analysis demonstrates that improving these parameters significantly reduces production costs, although their influence diminishes beyond certain points.

Moreover, environmental impacts of geological hydrogen are comparatively low, with a lifecycle greenhouse gas emission estimate of 0.4 kg CO_2e per kg of H_2 produced, underscoring its potential as a low-carbon hydrogen source. This positions geological hydrogen well to leverage regulatory incentives similar to those of the U.S. Inflation Reduction Act (IRA), which offers tax credits for hydrogen with low lifecycle emissions.

The results demonstrate that while natural hydrogen production is more cost-effective, its scalability is limited by the challenge of locating viable deposits, which is inherently uncertain. SGH, despite being more capital-intensive, offers significant advantages in terms of scalability, given the widespread occurrence of iron-rich rocks and the potential to control production rates. This makes SGH more favorable for co-location near demand centers, which can substantially improve economic viability by reducing transportation costs. The findings of this study emphasize the importance of strategic co-location, particularly for SGH, as hydrogen transportation is one of the most significant factors in scaling the hydrogen economy. The higher probability of finding iron-rich rocks near demand centers compared to GH deposits suggests that SGH projects could be developed to optimize proximity to hydrogen consumers, thereby enhancing the overall economics of production.

The TEA relies on several assumptions drawn from analogs in the natural gas and geothermal industries, given the limited public data available on geological hydrogen production. These assumptions include wellhead gas composition and production flow rates as well as CAPEX and OPEX derived from similar subsurface extraction technologies. While these analogs provide a reliable starting point for analysis, they introduce uncertainties that should be validated through dedicated field trials and pilot projects. The analysis also makes several assumptions regarding containment efficiency and serpentinization efficiency. The containment efficiency of injected water within the stimulation volume, is based on analogs from other fluid injection processes like enhanced geothermal systems and water flooding. Similarly, serpentinization efficiency, a key factor for SGH production, was assumed based on laboratory-scale experiments. These parameters must be refined with site-specific field data to accurately predict the outcomes of large-scale SGH projects.

Future work should focus on gathering more field data, particularly on wellhead production rates, gas compositions, and serpentinization efficiency, to validate the assumptions made in this analysis and reduce associated uncertainties. Additionally, exploring disposable catalysts and enhanced techniques for stimulating hydrogen production in less-than-ideal field conditions could further improve the economic feasibility of SGH.

In conclusion, while both natural and stimulated geological hydrogen present viable options for contributing to a sustainable energy future, practical considerations such as resource availability, production control, and scalability make SGH a particularly attractive option for long-term hydrogen production, especially when co-located with demand centers. The low environmental impact and potential cost-effectiveness of geological hydrogen production, combined with policy incentives, position it as a promising candidate in the global effort to transition to a low-carbon energy system.

Acknowledgement
We acknowledge funding from the sponsors of Stanford's Natural Gas Initiative (NGI) and the Stanford Center for Earth Resources Forecasting (SCERF).

References

[1] C. C. Elam, C. E. Gregoire PadrÃ, G. Sandrock, A. Luzzi, P. Lindblad, and E. Fjermestad Hagen, "Realizing the hydrogen future: the International Energy Agency's efforts to advance hydrogen energy technologies," *Int. J. Hydrogen Energy*, vol. 28, pp. 601–607, 2003.

[2] R. Moliner, M. J. Lázaro, and I. Suelves, "Analysis of the strategies for bridging the gap towards the Hydrogen Economy," *Int. J. Hydrogen Energy*, vol. 41, no. 43, pp. 19500–19508, Nov. 2016, doi: 10.1016/J.IJHYDENE.2016.06.202.

[3] C. Rigollet and A. Prinzhofer, "Natural Hydrogen: A New Source of Carbon-Free and Renewable Energy That Can Compete With Hydrocarbons," *First Break*, vol. 40, no. 10, pp. 78–84, Oct. 2022, doi: 10.3997/1365-2397.fb2022087.

[4] H. C. Petersen, "Does natural hydrogen exist?," *Int. J. Hydrogen Energy*, vol. 15, no. 1, p. 55, Jan. 1990, doi: 10.1016/0360-3199(90)90130-Q.

[5] C. Neal and G. Stanger, "Hydrogen generation from mantle source rocks in Oman," *Earth Planet. Sci. Lett.*, vol. 66, no. C, pp. 315–320, 1983, doi: 10.1016/0012-821X(83)90144-9.

[6] C. Vacquand, E. Deville, V. Beaumont, *et al.*, "Reduced gas seepages in ophiolitic complexes: Evidences for multiple origins of the H2-CH4-N2 gas mixtures," *Geochim. Cosmochim. Acta*, vol. 223, pp. 437–461, Feb. 2018, doi: 10.1016/J.GCA.2017.12.018.

[7] E. Deville and A. Prinzhofer, "The origin of N2-H2-CH4-rich natural gas seepages in ophiolitic context: A major and noble gases study of fluid seepages in New Caledonia," *Chem. Geol.*, vol. 440, pp. 139–147, Nov. 2016, doi: 10.1016/J.CHEMGEO.2016.06.011.

[8] R. N. Greenberger, J. F. Mustard, E. A. Cloutis, *et al.*, "Serpentinization, iron oxidation, and aqueous conditions in an ophiolite: Implications for hydrogen production and habitability on Mars," *Earth Planet. Sci. Lett.*, vol. 416, pp. 21–34, Apr. 2015, doi: 10.1016/j.epsl.2015.02.002.

[9] T. A. Abrajano, N. C. Sturchio, B. M. Kennedy, G. L. Lyon, K. Muehlenbachs, and J. K. Bohlke, "Geochemistry of reduced gas related to serpentinization of the Zambales ophiolite, Philippines," *Appl. Geochemistry*, vol. 5, no. 5–6, pp. 625–630, Sep. 1990, doi: 10.1016/0883-2927(90)90060-I.

[10] V. Zgonnik, "The occurrence and geoscience of natural hydrogen: A comprehensive review," Apr. 01, 2020, *Elsevier B.V.* doi: 10.1016/j.earscirev.2020.103140.

[11] J. Parnell and N. Blamey, "Global hydrogen reservoirs in basement and basins," *Geochem. Trans.*, vol. 18, no. 1, pp. 1–8, 2017, doi: 10.1186/s12932-017-0041-4.

[12] B. S. Lollar, T. C. Onstott, G. Lacrampe-Couloume, and C. J. Ballentine, "The contribution of the Precambrian continental lithosphere to global H2 production," *Nature*, vol. 516, no. 7531, pp. 379–382, Dec. 2014, doi: 10.1038/nature14017.

[13] V. N. Rumyantsev, "Hydrogen in the earth's outer core, and its role in the deep earth geodynamics," *Geodyn. Tectonophys.*, vol. 7, no. 1, pp. 119–135, Mar. 2016, doi: 10.5800/GT-2016-7-1-0200.

[14] E. I. Isaev, N. V Skorodumova, R. Ahuja, Y. K. Vekilov, and B. Rje Johansson, "Dynamical stability of Fe-H in the Earth's mantle and core regions," *PNAS*, vol. 104, no.

22, pp. 9168–9171, 2007.
[15] S. Tagawa, N. Sakamoto, K. Hirose, *et al.*, "Experimental evidence for hydrogen incorporation into Earth's core," *Nat. Commun.*, vol. 12, no. 1, Dec. 2021, doi: 10.1038/s41467-021-22035-0.
[16] C. J. Boreham, D. S. Edwards, K. Czado, *et al.*, "Hydrogen in Australian natural gas: occurrences, sources and resources," *APPEA J.*, vol. 61, no. 1, p. 163, 2021, doi: 10.1071/aj20044.
[17] E. C. Gaucher, "New perspectives in the industrial exploration for native hydrogen," Feb. 01, 2020, *Mineralogical Society of America*. doi: 10.2138/gselements.16.1.8.
[18] F. Klein, W. Bach, and T. M. McCollom, "Compositional controls on hydrogen generation during serpentinization of ultramafic rocks," *Lithos*, vol. 178, pp. 55–69, 2013, doi: 10.1016/j.lithos.2013.03.008.
[19] F. Osselin, C. Soulaine, C. Fauguerolles, E. C. Gaucher, B. Scaillet, and M. Pichavant, "Orange hydrogen is the new green," *Nat. Geosci.*, vol. 15, no. 10, pp. 765–769, 2022, doi: 10.1038/s41561-022-01043-9.
[20] A. Prinzhofer, C. S. Tahara Cissé, and A. B. Diallo, "Discovery of a large accumulation of natural hydrogen in Bourakebougou (Mali)," *Int. J. Hydrogen Energy*, vol. 43, no. 42, pp. 19315–19326, Oct. 2018, doi: 10.1016/j.ijhydene.2018.08.193.
[21] P. J. Ball and K. Czado, "Natural hydrogen: the new frontier," *Geoscientist*, 2022.
[22] O. Maiga, E. Deville, J. Laval, A. Prinzhofer, and A. B. Diallo, "Characterization of the spontaneously recharging natural hydrogen reservoirs of Bourakebougou in Mali," *Sci. Rep.*, vol. 13, no. 1, Dec. 2023, doi: 10.1038/s41598-023-38977-y.
[23] A. R. Brandt, "Greenhouse gas intensity of natural hydrogen produced from subsurface geologic accumulations," *Joule*, Jul. 2023, doi: 10.1016/j.joule.2023.07.001.
[24] Q. ning Tian, S. qing Yao, M. juan Shao, W. Zhang, and H. hua Wang, "Origin, discovery, exploration and development status and prospect of global natural hydrogen under the background of 'carbon neutrality,'" Oct. 2022, *KeAi Communications Co.* doi: 10.31035/cg2022046.
[25] J. C. Robins, D. Kesseli, E. Witter, and G. Rhodes, "2022 GETEM Geothermal Drilling Cost Curve Update," *Trans. - Geotherm. Resour. Counc.*, vol. 46, no. December, pp. 2029–2040, 2022.
[26] S. Mokhatab, W. A. Poe, and J. Y. Mak, *Handbook of natural gas transmission and processing: principles and practices*. Gulf professional publishing, 2018.
[27] "Building the Gulf Coast Clean Hydrogen Market: Summary of Public Workshop & Private Roundtable.," *Energy Futures Initiative*, 2022.
[28] E. S. Menon, *Gas pipeline hydraulics*. Crc Press, 2005.
[29] M. Azuma, K. Oimatsu, S. Oyama, *et al.*, "Safety design of compressed hydrogen trailers with composite cylinders," *Int. J. Hydrogen Energy*, vol. 39, no. 35, pp. 20420–20425, 2014.
[30] Bayo Tech, "HyFill^{TM} Bulk Hydrogen Transport Trailers," 2022.
[31] J. Guélard, V. Beaumont, V. Rouchon, *et al.*, "Natural H 2 in Kansas: Deep or shallow origin?," vol. 18, no. 5, pp. 1841–1865, 2017, doi: 10.1002/2016GC006544ï.
[32] A. Brown, "Origin of helium and nitrogen in the Panhandle-Hugoton field, Texas, Oklahoma, and Kansas, USA," *Am. Assoc. Pet. Geol. Bull.*, no. 20,180,713, 2018.
[33] R. F. Broadhead, "Helium in New Mexico—geologic distribution, resource demand, and exploration possibilities," *New Mex. Geol.*, vol. 27, no. 4, pp. 93–101, 2005.

[34] E. Grynia and P. J. Griffin, “Helium in natural gas-occurrence and production,” *J. Nat. Gas Eng.*, vol. 1, no. 2, pp. 163–215, 2016.
[35] A. Zolfaghari, J. Gehman, and D. S. Alessi, “Cost analysis of wastewater production from conventional and unconventional oil and gas wells,” *Fuel*, vol. 323, p. 124222, 2022.
[36] M. Netusil and P. Ditl, “Comparison of three methods for natural gas dehydration,” *J. Nat. gas Chem.*, vol. 20, no. 5, pp. 471–476, 2011.
[37] M. R. Rahimpour, M. A. Makarem, and M. Meshksar, *Advances in Natural Gas: Formation, Processing, and Applications. Volume 2: Natural Gas Sweetening*. Elsevier, 2024.
[38] G. Liu, L. Zhu, J. Hong, and H. Liu, “Technical, Economical, and Environmental Performance Assessment of an Improved Triethylene Glycol Dehydration Process for Shale Gas,” *ACS omega*, vol. 7, no. 2, pp. 1861–1873, 2022.
[39] J. Wills, M. Shemaria, and M. J. Mitariten, “Production of pipeline-quality natural gas with the molecular gate CO2 removal process,” *SPE Prod. Facil.*, vol. 19, no. 01, pp. 4–8, 2004.
[40] H. M. Lamadrid, J. D. Rimstidt, E. M. Schwarzenbach, *et al.*, “Effect of water activity on rates of serpentinization of olivine,” *Nat. Commun.*, vol. 8, Jul. 2017, doi: 10.1038/ncomms16107.
[41] H. M. Miller, L. E. Mayhew, E. T. Ellison, P. Kelemen, M. Kubo, and A. S. Templeton, “Low temperature hydrogen production during experimental hydration of partially-serpentinized dunite,” *Geochim. Cosmochim. Acta*, vol. 209, pp. 161–183, 2017, doi: 10.1016/j.gca.2017.04.022.
[42] A. R. Kovscek, “Emerging challenges and potential futures for thermally enhanced oil recovery,” *J. Pet. Sci. Eng.*, vol. 98–99, pp. 130–143, 2012, doi: 10.1016/j.petrol.2012.08.004.
[43] R. Huang, W. Sun, M. Song, and X. Ding, “Influence of ph on molecular hydrogen (H2) generation and reaction rates during serpentinization of peridotite and olivine,” *Minerals*, vol. 9, no. 11, 2019, doi: 10.3390/min9110661.
[44] E. S. Boyd, D. R. Colman, and A. S. Templeton, “Perspective: Microbial hydrogen metabolism in rock-hosted ecosystems,” *Front. Energy Res.*, vol. 12, no. March, pp. 1–8, 2024, doi: 10.3389/fenrg.2024.1340410.
[45] S. Barbier, F. Huang, M. Andreani, *et al.*, “A review of H2, CH4, and hydrocarbon formation in experimental serpentinization using network analysis,” *Front. Earth Sci.*, vol. 8, p. 209, 2020.
[46] T. M. McCollom, F. Klein, M. Robbins, *et al.*, “Temperature trends for reaction rates, hydrogen generation, and partitioning of iron during experimental serpentinization of olivine,” *Geochim. Cosmochim. Acta*, vol. 181, pp. 175–200, 2016, doi: 10.1016/j.gca.2016.03.002.
[47] T. D. Ely, J. M. Leong, P. A. Canovas, and E. L. Shock, “Huge Variation in H2 Generation During Seawater Alteration of Ultramafic Rocks,” *Geochemistry, Geophys. Geosystems*, vol. 24, no. 3, pp. 1–23, 2023, doi: 10.1029/2022GC010658.
[48] A. S. Templeton, E. T. Ellison, P. B. Kelemen, *et al.*, “Low-temperature hydrogen production and consumption in partially-hydrated peridotites in Oman: implications for stimulated geological hydrogen production,” *Front. Geochemistry*, vol. 2, pp. 1–20, 2024, doi: 10.3389/fgeoc.2024.1366268.
[49] U.S.E.I.A., “Short-Term Energy Outlook,” 2023.

[50] C. Yang and J. Ogden, "Determining the lowest-cost hydrogen delivery mode," *Int. J. Hydrogen Energy*, vol. 32, no. 2, pp. 268–286, 2007, doi: 10.1016/j.ijhydene.2006.05.009.
[51] N. S. Muhammed, A. O. Gbadamosi, E. I. Epelle, *et al.*, "Hydrogen production, transportation, utilization, and storage: Recent advances towards sustainable energy," *J. Energy Storage*, vol. 73, no. PD, p. 109207, 2023, doi: 10.1016/j.est.2023.109207.
[52] DOE, "Pathways to Commercial Liftoff: Clean Hydrogen," 2023.
[53] G. Hydrogen, "Committed to developing naturally occurring Hydrogen and Helium in Australia." [Online]. Available: https://www.goldhydrogen.com.au/wp/wp-content/uploads/2024.10.21-AGM-Presentation.pdf
[54] M. Sand, R. B. Skeie, M. Sandstad, *et al.*, "A multi-model assessment of the Global Warming Potential of hydrogen," *Commun. Earth Environ.*, vol. 4, no. 1, Dec. 2023, doi: 10.1038/s43247-023-00857-8.
[55] R. Derwent, P. Simmonds, S. O'Doherty, A. Manning, W. Collins, and D. Stevenson, "Global environmental impacts of the hydrogen economy," *Int. J. Nucl. Hydrog. Prod. Appl.*, vol. 1, no. 1, p. 57, 2006, doi: 10.1504/ijnhpa.2006.009869.

Supplementary Information [****depending on the journal and their formatting requirements, SI might be at the end, after the reference section***]

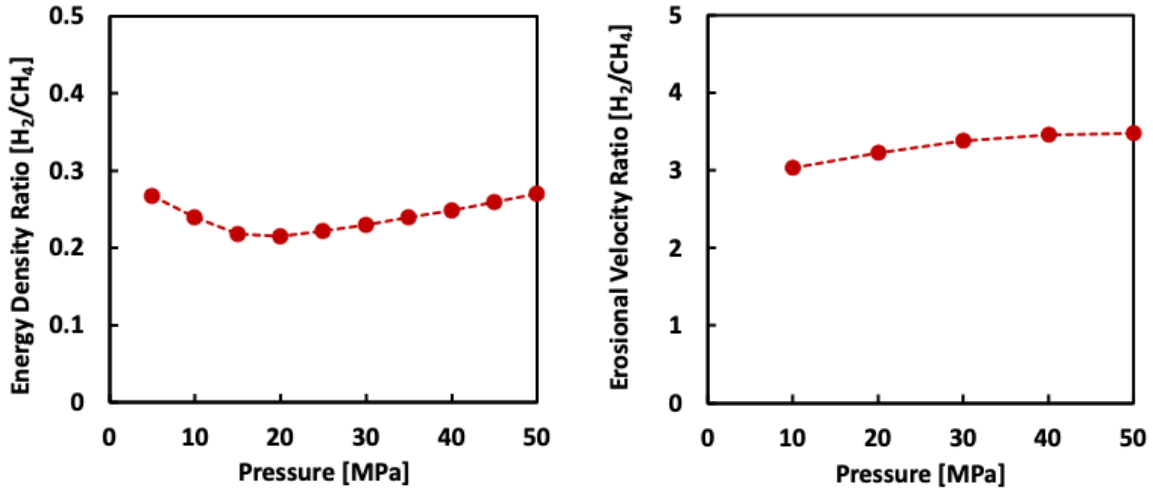

Figure S.1: *(left) Energy density ratio of hydrogen to methane at 20°C. (right) Erosional velocity ratio of hydrogen to methane at 20°C.*

Erosional Velocity Formula:

$$u_{erosional} = 100\sqrt{\frac{ZRT}{29GP}}$$

Where Z is the compressibility factor of the gas, R is the gas constant, T is the gas temperature, G is the gas gravity, and P is the gas pressure [28].

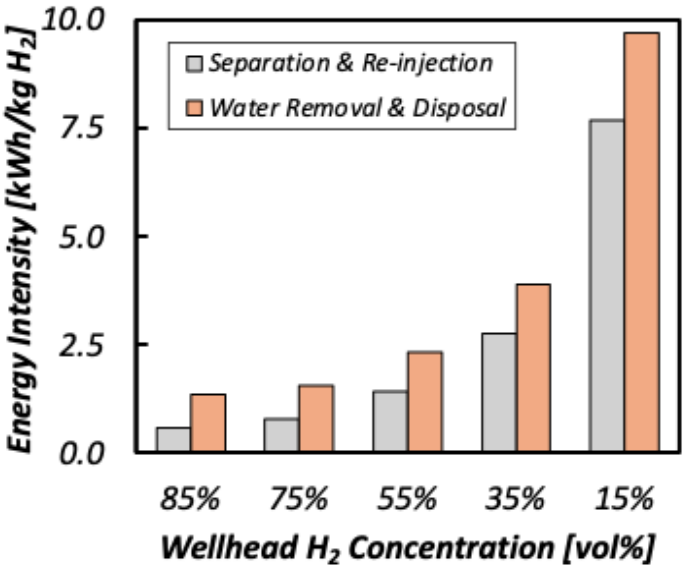

Fig- S.2: *Energy intensity of the two primary cost drivers for surface level processing of raw GH, which includes separation and re-injection costs for the PSA system, as well as water removal to achieve acceptable moisture levels*

	Units	FLSH-GAS	H2-PROD	INJECT	L-TEG-1	L-TEG-2	S1	S3	S4	S5	S6	S8	S10	S11	S13
Phase		Vapor Phase	Vapor Phase	Vapor Phase	Liquid Phase	Liquid Phase	Vapor Phase		Vapor Phase		Vapor Phase	Vapor Phase		Vapor Phase	
Temperature	C	1.20E+02	5.00E+01	5.00E+01	5.88E+01	5.00E+01	3.09E+01	4.00E+01	4.00E+01	4.25E+01	4.57E+01	4.58E+01	4.57E+01	4.16E+01	1.20E+02
Pressure	bar	7.00E+00	3.00E+01	7.00E+00	3.00E+01	3.00E+01	7.00E+00	3.00E+01	3.00E+01	7.00E+00	3.00E+01	2.70E+01	3.00E+01	1.00E+00	7.00E+00
Molar Vapor Fraction		1.00E+00	1.00E+00	1.00E+00	0.00E+00	0.00E+00	1.00E+00	9.97E-01	1.00E+00	5.99E-03	1.00E+00	1.00E+00	1.00E+00	1.00E+00	7.46E-03
Molar Liquid Fraction		0.00E+00	0.00E+00	0.00E+00	1.00E+00	1.00E+00	0.00E+00	2.85E-03	0.00E+00	9.94E-01	0.00E+00	0.00E+00	4.52E-07	0.00E+00	9.93E-01
Molar Solid Fraction		0.00E+00	0.00E+00	0.00E+00	0.00E+00	0.00E+00	0.00E+00	0.00E+00	0.00E+00	0.00E+00	0.00E+00	0.00E+00	0.00E+00	0.00E+00	0.00E+00
Mass Vapor Fraction		1.00E+00	1.00E+00	1.00E+00	0.00E+00	0.00E+00	1.00E+00	9.93E-01	1.00E+00	5.83E-04	1.00E+00	1.00E+00	1.00E+00	1.00E+00	9.58E-04
Mass Liquid Fraction		0.00E+00	0.00E+00	0.00E+00	1.00E+00	1.00E+00	0.00E+00	6.93E-03	0.00E+00	9.99E-01	0.00E+00	0.00E+00	4.18E-06	1.60E-13	9.99E-01
Mass Solid Fraction		0.00E+00	0.00E+00	0.00E+00	0.00E+00	0.00E+00	0.00E+00	0.00E+00	0.00E+00	0.00E+00	0.00E+00	0.00E+00	0.00E+00	0.00E+00	0.00E+00
Molar Enthalpy	MJ/kmol	-9.73E+01	5.83E-01	3.72E+01	-8.61E+02	-7.81E+02	-1.59E+01	-1.58E+01	-1.59E+01	-7.45E+02	1.42E+01	3.75E-01	-3.75E+01	-3.75E+01	7.43E+02
Mass Enthalpy	kJ/kg	-5.63E+03	2.39E+02	-2.37E+03	-5.31E+03	-4.38E+03	-2.15E+03	-2.13E+03	-2.03E+03	-4.42E+03	-1.93E+03	1.80E+02	-2.39E+03	-2.39E+03	-4.26E+03
Enthalpy Flow	kJ/hr	-4.27E+04	4.15E+05	-1.82E+07	-4.27E+07	-3.39E+07	-2.13E+07	-2.13E+07	-2.02E+07	-4.38E+07	-1.90E+07	3.12E+06	-1.84E+07	-1.84E+07	-4.25E+07
Average MW		1.77E+01	2.10E+00	1.57E+01	1.80E+02	1.65E+02	7.48E+00	7.48E+00	7.37E+00	1.41E+02	7.33E+00	2.10E+00	1.57E+01	1.57E+01	1.41E+02
Total Mole Flows	kmol/hr	4.38E-01	8.25E+02	5.17E+02	5.33E+01	5.54E+01	1.35E+03	1.35E+03	1.35E+03	5.72E+01	1.34E+03	8.25E+02	5.17E+02	5.17E+02	5.73E+01
H2	kmol/hr	1.56E-01	8.22E+02	2.06E+02	0.00E+00	1.67E-04	1.03E+03	1.03E+03	1.03E+03	1.92E-01	1.03E+03	8.22E+02	2.06E+02	2.06E+02	1.95E-01
CH4	kmol/hr	1.18E-01	1.23E+00	1.22E+02	0.00E+00	5.41E-03	1.23E+02	1.23E+02	1.23E+02	2.74E-01	1.23E+02	1.23E+00	1.22E+02	1.22E+02	2.74E-01
N2	kmol/hr	6.40E-02	1.64E+00	1.63E+02	0.00E+00	2.89E-04	1.64E+02	1.64E+02	1.64E+02	9.46E-02	1.64E+02	1.64E+00	1.63E+02	1.63E+02	9.46E-02
H2O	kmol/hr	2.31E-02	1.72E-03	1.30E-01	0.00E+00	2.10E+00	6.97E+00	6.97E+00	3.13E+00	3.01E+00	1.22E-01	1.92E-03	1.20E-01	1.20E-01	3.01E+00
H2S	kmol/hr	0.00E+00	0.00E+00	0.00E+00	0.00E+00	0.00E+00	0.00E+00	0.00E+00	0.00E+00	0.00E+00	0.00E+00	0.00E+00	0.00E+00	0.00E+00	0.00E+00
HE	kmol/hr	0.00E+00	0.00E+00	0.00E+00	0.00E+00	0.00E+00	0.00E+00	0.00E+00	0.00E+00	0.00E+00	0.00E+00	0.00E+00	0.00E+00	0.00E+00	0.00E+00
CO2	kmol/hr	7.62E-02	2.79E-01	2.67E+01	0.00E+00	3.25E-02	2.74E+01	2.74E+01	2.74E+01	4.04E-01	2.76E+01	2.76E-01	2.67E+01	2.67E+01	4.04E-01
CO	kmol/hr	0.00E+00	0.00E+00	0.00E+00	0.00E+00	0.00E+00	0.00E+00	0.00E+00	0.00E+00	0.00E+00	0.00E+00	0.00E+00	0.00E+00	0.00E+00	0.00E+00
TEG	kmol/hr	1.25E-04	0.00E+00	4.65E-04	5.33E+01	5.33E+01	0.00E+00	0.00E+00	0.00E+00	5.33E+01	4.65E-04	0.00E+00	4.65E-04	4.65E-04	5.33E+01
Mole Fractions															
H2	-	3.61E-01	9.96E-01	3.98E-01	0.00E+00	1.93E-06	7.61E-01	7.61E-01	7.64E-01	3.35E-03	7.68E-01	9.96E-01	3.98E-01	3.98E-01	3.35E-03
CH4	-	2.68E-01	1.48E-03	2.36E-01	0.00E+00	9.78E-05	9.14E-02	9.14E-02	9.12E-02	4.79E-03	9.17E-02	1.48E-03	2.36E-01	2.36E-01	4.79E-03
N2	-	1.46E-01	1.99E-03	3.16E-01	0.00E+00	5.22E-06	1.22E-01	1.22E-01	1.22E-01	1.65E-03	1.22E-01	1.99E-03	3.15E-01	3.15E-01	1.65E-03
H2O	-	5.27E-02	2.07E-06	2.53E-04	0.00E+00	3.79E-02	5.17E-03	5.17E-03	2.33E-03	5.26E-02	9.07E-05	1.47E-06	2.33E-04	2.33E-04	5.26E-02
H2S	-	0.00E+00	0.00E+00	0.00E+00	0.00E+00	0.00E+00	0.00E+00	0.00E+00	0.00E+00	0.00E+00	0.00E+00	0.00E+00	0.00E+00	0.00E+00	0.00E+00
HE	-	0.00E+00	0.00E+00	0.00E+00	0.00E+00	0.00E+00	0.00E+00	0.00E+00	0.00E+00	0.00E+00	0.00E+00	0.00E+00	0.00E+00	0.00E+00	0.00E+00
CO2	-	1.72E-01	3.37E-04	5.17E-02	0.00E+00	5.87E-04	2.03E-02	2.03E-02	2.04E-02	7.05E-03	2.01E-02	3.37E-04	5.17E-02	5.17E-02	7.05E-03
CO	-	0.00E+00	0.00E+00	0.00E+00	0.00E+00	0.00E+00	0.00E+00	0.00E+00	0.00E+00	0.00E+00	0.00E+00	0.00E+00	0.00E+00	0.00E+00	0.00E+00
TEG	-	2.93E-04	0.00E+00	9.00E-07	1.00E+00	9.61E-01	0.00E+00	0.00E+00	0.00E+00	9.31E-01	3.47E-07	0.00E+00	9.00E-07	9.00E-07	9.31E-01
Total Mass Flows	kg/hr	7.74E+00	1.73E+03	8.11E+03	8.00E+03	8.04E+03	9.99E+03	9.99E+03	9.92E+03	8.08E+03	9.84E+03	1.73E+03	8.11E+03	8.11E+03	8.08E+03
H2	kg/hr	3.15E-01	1.66E+03	4.14E+02	0.00E+00	2.38E-04	2.07E+03	2.07E+03	2.08E+03	3.86E-01	2.07E+03	1.66E+03	4.14E+02	4.14E+02	3.86E-01
CH4	kg/hr	1.88E+00	1.97E+01	1.95E+03	0.00E+00	8.67E-02	1.96E+03	1.96E+03	1.96E+03	4.40E+00	1.97E+03	1.97E+01	1.95E+03	1.95E+03	4.40E+00
N2	kg/hr	1.79E+00	4.60E+01	4.58E+03	0.00E+00	8.09E-03	4.61E+03	4.61E+03	4.61E+03	2.65E+00	4.60E+03	4.60E+01	4.58E+03	4.58E+03	2.65E+00
H2O	kg/hr	4.16E-01	2.19E-02	2.17E+00	0.00E+00	3.78E+01	1.26E+02	1.26E+02	5.64E+01	5.42E+01	2.19E+00	2.19E-02	2.17E+00	2.17E+00	5.42E+01
H2S	kg/hr	0.00E+00	0.00E+00	0.00E+00	0.00E+00	0.00E+00	0.00E+00	0.00E+00	0.00E+00	0.00E+00	0.00E+00	0.00E+00	0.00E+00	0.00E+00	0.00E+00
HE	kg/hr	0.00E+00	0.00E+00	0.00E+00	0.00E+00	0.00E+00	0.00E+00	0.00E+00	0.00E+00	0.00E+00	0.00E+00	0.00E+00	0.00E+00	0.00E+00	0.00E+00
CO2	kg/hr	3.35E+00	1.19E+01	1.18E+03	0.00E+00	1.43E+00	1.21E+03	1.21E+03	1.21E+03	1.78E+01	1.19E+03	1.19E+01	1.18E+03	1.18E+03	1.78E+01
CO	kg/hr	0.00E+00	0.00E+00	0.00E+00	0.00E+00	0.00E+00	0.00E+00	0.00E+00	0.00E+00	0.00E+00	0.00E+00	0.00E+00	0.00E+00	0.00E+00	0.00E+00
TEG	kg/hr	1.93E-02	0.00E+00	6.99E-02	8.00E+03	8.00E+03	0.00E+00	0.00E+00	0.00E+00	8.00E+03	6.99E-02	0.00E+00	6.99E-02	6.99E-02	8.00E+03
Mass Fractions															
H2	-	4.12E-02	9.59E-01	5.11E-02	0.00E+00	2.96E-08	2.07E-01	2.07E-01	2.09E-01	4.78E-05	2.14E-01	9.59E-01	5.11E-02	5.11E-02	4.78E-05
CH4	-	2.44E-01	1.14E-02	2.41E-01	0.00E+00	1.08E-05	1.96E-01	1.96E-01	1.96E-01	5.44E-04	2.01E-01	1.14E-02	2.41E-01	2.41E-01	5.44E-04
N2	-	2.32E-01	2.65E-02	5.62E-01	0.00E+00	1.03E-06	4.61E-01	4.61E-01	4.64E-01	3.28E-04	4.68E-01	2.65E-02	5.62E-01	5.62E-01	3.28E-04
H2O	-	5.38E-02	1.36E-05	2.68E-04	0.00E+00	4.71E-03	1.26E-02	1.26E-02	5.66E-03	6.71E-03	2.23E-04	1.26E-05	2.68E-04	2.68E-04	6.71E-03
H2S	-	0.00E+00	0.00E+00	0.00E+00	0.00E+00	0.00E+00	0.00E+00	0.00E+00	0.00E+00	0.00E+00	0.00E+00	0.00E+00	0.00E+00	0.00E+00	0.00E+00
HE	-	0.00E+00	0.00E+00	0.00E+00	0.00E+00	0.00E+00	0.00E+00	0.00E+00	0.00E+00	0.00E+00	0.00E+00	0.00E+00	0.00E+00	0.00E+00	0.00E+00
CO2	-	4.27E-01	6.85E-03	1.46E-01	0.00E+00	1.78E-04	1.21E-01	1.21E-01	1.22E-01	2.20E-03	1.21E-01	6.85E-03	1.45E-01	1.45E-01	2.20E-03
CO	-	0.00E+00	0.00E+00	0.00E+00	0.00E+00	0.00E+00	0.00E+00	0.00E+00	0.00E+00	0.00E+00	0.00E+00	0.00E+00	0.00E+00	0.00E+00	0.00E+00
TEG	-	2.49E-03	0.00E+00	8.62E-06	1.00E+00	9.95E-01	0.00E+00	0.00E+00	0.00E+00	9.90E-01	7.16E-06	0.00E+00	8.62E-06	8.62E-06	9.90E-01
Volume Flow	l/min	3.41E+01	1.25E+04	3.31E+04	1.19E+02	1.20E+02	8.13E+04	1.97E+04	1.97E+04	1.42E+02	2.00E+04	1.37E+04	7.61E+03	2.25E+05	1.62E+02

	Units	S14	S15	S16	S17	S18	S19	S20	S21	TEG-MKUP	WELLHEAD	WW-1	WW-2	WW-3	WW-OUT
Phase		Liquid Phase	Liquid Phase	Liquid Phase	Vapor Phase	Liquid Phase	Liquid Phase	Liquid Phase	Liquid Phase	Liquid Phase		Liquid Phase	Liquid Phase	Vapor Phase	
Temperature	C	1.20E+02	1.90E+02	1.88E+02	2.65E+02	2.05E+02	1.36E+02	1.36E+02	1.36E+02	2.00E+01	3.00E+01	3.00E+01	4.00E+01	9.99E+01	5.19E+01
Pressure	bar	7.00E+00	7.00E+00	1.50E+00	1.50E+00	1.50E+00	1.50E+00	1.50E+00	3.00E+01	1.50E+00	7.00E+00	7.00E+00	3.00E+01	1.50E+00	1.50E+00
Molar Vapor Fraction		0.00E+00	7.49E-04	0.00E+00	1.00E+00	0.00E+00	0.00E+00	0.00E+00	0.00E+00	0.00E+00	9.85E-01	0.00E+00	0.00E+00	1.00E+00	2.20E-02
Molar Liquid Fraction		1.00E+00	9.99E-01	1.00E+00	0.00E+00	1.00E+00	1.00E+00	1.00E+00	1.00E+00	1.00E+00	1.48E-02	1.00E+00	1.00E+00	0.00E+00	9.78E-01
Molar Solid Fraction		0.00E+00	0.00E+00	0.00E+00	0.00E+00	0.00E+00	0.00E+00	0.00E+00	0.00E+00	0.00E+00	0.00E+00	0.00E+00	0.00E+00	0.00E+00	0.00E+00
Mass Vapor Fraction		0.00E+00	1.23E-04	0.00E+00	1.00E+00	0.00E+00	0.00E+00	0.00E+00	0.00E+00	0.00E+00	9.64E-01	0.00E+00	0.00E+00	1.00E+00	3.94E-02
Mass Liquid Fraction		1.00E+00	1.00E+00	1.00E+00	0.00E+00	1.00E+00	1.00E+00	1.00E+00	1.00E+00	1.00E+00	3.55E-02	1.00E+00	1.00E+00	0.00E+00	9.61E-01
Mass Solid Fraction		0.00E+00	0.00E+00	0.00E+00	0.00E+00	0.00E+00	0.00E+00	0.00E+00	0.00E+00	0.00E+00	0.00E+00	0.00E+00	0.00E+00	0.00E+00	0.00E+00
Molar Enthalpy	MJ/kmol	-7.29E+02	-7.36E+02	-7.36E+02	-7.32E+02	-7.93E+02	-7.88E+02	-7.88E+02	-7.84E+02	-4.18E+02	-2.00E+01	-2.47E+02	-2.84E+02	-2.48E+02	-2.83E+02
Mass Enthalpy	kJ/kg	-5.36E+03	-5.10E+03	-5.09E+03	-9.23E+03	-5.04E+03	-5.30E+03	-5.30E+03	-5.26E+03	-5.30E+03	-2.64E+03	-1.93E+04	-1.93E+04	-1.93E+04	-1.95E+04
Enthalpy Flow	kJ/hr	-4.15E+07	-4.12E+07	-4.09E+07	-4.61E+04	-4.05E+07	-4.18E+07	-4.18E+07	-4.18E+07	-4.18E+04	-2.73E+07	-5.87E+06	-1.93E+06	-3.45E+05	-7.32E+06
Average MW		1.42E+02	1.42E+02	1.45E+02	2.87E+01	1.45E+02	1.45E+02	1.45E+02	1.45E+02	1.50E+02	7.56E+00	1.80E+01	1.80E+01	2.40E+01	1.83E+01
Total Mole Flows	kmol/hr	5.68E+01	5.68E+01	5.56E+01	1.48E-01	5.54E+01	5.54E+01	5.54E+01	5.54E+01	1.33E-02	1.37E+03	2.84E+01	3.84E+00	1.48E+00	2.57E+01
H2	kmol/hr	3.33E-02	3.33E-02	8.27E-04	5.20E-04	1.87E-04	1.07E-04	1.07E-04	1.07E-04	0.00E+00	1.03E+03	2.06E-05	2.31E-09	3.32E-02	3.32E-02
CH4	kmol/hr	1.96E-01	1.96E-01	1.20E-02	6.57E-03	5.41E-03	5.41E-03	5.41E-03	5.41E-03	0.00E+00	1.23E+02	1.37E-05	1.46E-05	1.51E-01	1.51E-01
N2	kmol/hr	3.06E-02	3.06E-02	1.68E-03	7.81E-04	2.95E-04	2.95E-04	2.95E-04	2.95E-04	0.00E+00	1.64E+02	2.01E-06	7.37E-06	3.03E-02	3.03E-02
H2O	kmol/hr	2.99E+00	2.99E+00	2.71E+00	1.10E-01	2.10E+00	2.10E+00	2.10E+00	2.10E+00	0.00E+00	2.74E+01	2.04E+01	3.84E+00	8.85E-01	2.52E+01
H2S	kmol/hr	0.00E+00	0.00E+00	0.00E+00	0.00E+00	0.00E+00	0.00E+00	0.00E+00	0.00E+00	0.00E+00	0.00E+00	0.00E+00	0.00E+00	0.00E+00	0.00E+00
HE	kmol/hr	0.00E+00	0.00E+00	0.00E+00	0.00E+00	0.00E+00	0.00E+00	0.00E+00	0.00E+00	0.00E+00	0.00E+00	0.00E+00	0.00E+00	0.00E+00	0.00E+00
CO2	kmol/hr	3.29E-01	3.29E-01	5.15E-02	1.90E-02	3.25E-02	3.25E-02	3.25E-02	3.25E-02	0.00E+00	2.74E+01	3.80E-05	3.38E-05	2.96E-01	2.96E-01
CO	kmol/hr	0.00E+00	0.00E+00	0.00E+00	0.00E+00	0.00E+00	0.00E+00	0.00E+00	0.00E+00	0.00E+00	0.00E+00	0.00E+00	0.00E+00	0.00E+00	0.00E+00
TEG	kmol/hr	5.33E+01	5.33E+01	5.33E+01	9.32E-03	5.33E+01	5.33E+01	5.33E+01	5.33E+01	1.33E-02	0.00E+00	0.00E+00	0.00E+00	9.43E-03	9.43E-03
Mole Fractions															
H2	-	5.85E-04	5.85E-04	1.13E-05	3.51E-03	1.93E-06	1.93E-06	1.93E-06	1.93E-06	0.00E+00	7.58E-01	1.01E-06	6.02E-06	2.36E-02	1.29E-03
CH4	-	2.75E-03	2.75E-03	2.16E-04	4.45E-02	9.76E-05	9.76E-05	9.76E-05	9.76E-05	0.00E+00	9.00E-02	6.80E-07	3.81E-06	1.08E-01	5.88E-03
N2	-	5.38E-04	5.38E-04	1.94E-05	5.34E-03	5.32E-06	5.32E-06	5.32E-06	5.32E-06	0.00E+00	1.20E-01	9.93E-08	6.17E-07	2.15E-02	1.18E-03
H2O	-	5.26E-02	5.26E-02	3.98E-02	7.53E-01	3.79E-02	3.79E-02	3.79E-02	3.79E-02	0.00E+00	2.00E-02	1.90E+00	1.00E+00	6.30E-01	9.80E-01
H2S	-	0.00E+00	0.00E+00	0.00E+00	0.00E+00	0.00E+00	0.00E+00	0.00E+00	0.00E+00	0.00E+00	0.00E+00	0.00E+00	0.00E+00	0.00E+00	0.00E+00
HE	-	0.00E+00	0.00E+00	0.00E+00	0.00E+00	0.00E+00	0.00E+00	0.00E+00	0.00E+00	0.00E+00	0.00E+00	0.00E+00	0.00E+00	0.00E+00	0.00E+00
CO2	-	5.78E-03	5.78E-03	9.27E-04	1.30E-01	5.87E-04	5.87E-04	5.87E-04	5.87E-04	0.00E+00	2.00E-02	1.98E-06	8.79E-06	2.11E-01	1.15E-02
CO	-	0.00E+00	0.00E+00	0.00E+00	0.00E+00	0.00E+00	0.00E+00	0.00E+00	0.00E+00	0.00E+00	0.00E+00	0.00E+00	0.00E+00	0.00E+00	0.00E+00
TEG	-	9.38E-01	9.38E-01	9.59E-01	6.37E-02	9.61E-01	9.61E-01	9.61E-01	9.61E-01	1.00E+00	0.00E+00	0.00E+00	0.00E+00	6.72E-03	3.67E-04
Total Mass Flows	kg/hr	8.07E+03	8.07E+03	8.04E+03	4.35E+00	8.04E+03	8.04E+03	8.04E+03	8.04E+03	2.00E+00	1.04E+04	3.68E+02	6.91E+01	3.37E+01	4.71E+02
H2	kg/hr	6.70E-02	6.70E-02	1.26E-03	1.05E-03	2.36E-04	2.16E-04	2.36E-04	2.16E-04	0.00E+00	2.07E+03	4.15E-05	4.67E-05	6.68E-02	6.68E-02
CH4	kg/hr	2.51E+00	2.51E+00	1.92E-01	1.05E-01	8.67E-02	8.67E-02	8.67E-02	8.67E-02	0.00E+00	1.98E+03	2.19E-04	2.35E-04	2.42E+00	2.42E+00
N2	kg/hr	8.56E-01	8.56E-01	3.01E-02	2.19E-02	8.25E-03	8.25E-03	8.25E-03	8.25E-03	0.00E+00	4.61E+03	5.66E-05	6.64E-05	8.48E-01	8.48E-01
H2O	kg/hr	5.38E+01	5.38E+01	3.98E+01	1.38E+00	3.78E+01	3.78E+01	3.78E+01	3.78E+01	0.00E+00	4.94E+02	3.68E+02	6.92E+01	1.59E+01	4.53E+02
H2S	kg/hr	0.00E+00	0.00E+00	0.00E+00	0.00E+00	0.00E+00	0.00E+00	0.00E+00	0.00E+00	0.00E+00	0.00E+00	0.00E+00	0.00E+00	0.00E+00	0.00E+00
HE	kg/hr	0.00E+00	0.00E+00	0.00E+00	0.00E+00	0.00E+00	0.00E+00	0.00E+00	0.00E+00	0.00E+00	0.00E+00	0.00E+00	0.00E+00	0.00E+00	0.00E+00
CO2	kg/hr	1.45E+01	1.45E+01	2.27E+00	8.35E-01	1.43E+00	1.43E+00	1.43E+00	1.43E+00	0.00E+00	1.21E+03	1.67E-03	1.49E-03	1.30E+01	1.30E+01
CO	kg/hr	0.00E+00	0.00E+00	0.00E+00	0.00E+00	0.00E+00	0.00E+00	0.00E+00	0.00E+00	0.00E+00	0.00E+00	0.00E+00	0.00E+00	0.00E+00	0.00E+00
TEG	kg/hr	8.00E+03	8.00E+03	8.00E+03	1.40E+00	8.00E+03	8.00E+03	8.00E+03	8.00E+03	2.00E+00	0.00E+00	0.00E+00	0.00E+00	1.42E+00	1.42E+00
Mass Fractions															
H2	-	8.31E-06	8.31E-06	1.67E-07	2.41E-04	2.89E-08	2.69E-08	2.89E-08	2.69E-08	0.00E+00	2.00E-01	1.13E-07	6.74E-07	1.98E-03	1.42E-04
CH4	-	3.11E-04	3.11E-04	2.39E-05	2.42E-02	1.08E-05	1.08E-05	1.08E-05	1.08E-05	0.00E+00	1.91E-01	5.95E-07	3.30E-06	7.19E-02	5.15E-03
N2	-	1.06E-04	1.06E-04	3.75E-06	5.03E-03	1.03E-06	1.03E-06	1.03E-06	1.03E-06	0.00E+00	4.45E-01	1.54E-07	9.58E-07	2.51E-02	1.86E-03
H2O	-	6.66E-03	6.66E-03	4.95E-03	4.57E-01	4.71E-03	4.71E-03	4.71E-03	4.71E-03	0.00E+00	4.77E-02	1.80E+00	1.00E+00	4.73E-01	9.62E-01
H2S	-	0.00E+00	0.00E+00	0.00E+00	0.00E+00	0.00E+00	0.00E+00	0.00E+00	0.00E+00	0.00E+00	0.00E+00	0.00E+00	0.00E+00	0.00E+00	0.00E+00
HE	-	0.00E+00	0.00E+00	0.00E+00	0.00E+00	0.00E+00	0.00E+00	0.00E+00	0.00E+00	0.00E+00	0.00E+00	0.00E+00	0.00E+00	0.00E+00	0.00E+00
CO2	-	1.79E-03	1.79E-03	2.82E-04	1.92E-01	1.78E-04	1.78E-04	1.78E-04	1.78E-04	0.00E+00	1.16E-01	4.54E-06	2.15E-05	3.86E-01	2.77E-02
CO	-	0.00E+00	0.00E+00	0.00E+00	0.00E+00	0.00E+00	0.00E+00	0.00E+00	0.00E+00	0.00E+00	0.00E+00	0.00E+00	0.00E+00	0.00E+00	0.00E+00
TEG	-	9.91E-01	9.91E-01	9.95E-01	3.22E-01	9.95E-01	9.95E-01	9.95E-01	9.95E-01	1.00E+00	0.00E+00	0.00E+00	0.00E+00	4.20E-02	3.01E-03
Volume Flow	l/min	1.28E+02	1.41E+02	1.39E+02	6.42E+01	1.38E+02	1.29E+02	1.29E+02	1.29E+02	2.91E-02	8.12E+04	6.20E+00	1.18E+00	4.88E+02	1.76E+02

Fig- S.3- *Energy and mass flow summary of each stream of the surface level processing modeled in ASPEN Plus*